



In silico scaffold evaluation and solid phase approach to identify new gelatinase inhibitors

Alessandra Topai^{a,*}, Perla Breccia^b, Franco Minissi^a, Alessandro Padova^c, Stefano Marini^d, Ilaria Cerbara^a

^a Colosseum Combinatorial Chemistry Centre for Technology (C4T S.C.a r.l.), Via della Ricerca Scientifica s.n.c., I-00133 Rome, Italy

^b BioFocus, Chesterford Research Park, UK-CB10 1XL Saffron Walden, United Kingdom

^c Molecular Informatics Dept, Siena Biotech S.p.A., Strada del Petriccio e Belriguardo, 35, I-53100 Siena, Italy

^d Department of Experimental Medicine and Biochemical Sciences, University of Roma Tor Vergata, Via Montpellier 1, I-00133 Roma, Italy

ARTICLE INFO

Article history:

Received 13 October 2011

Revised 2 February 2012

Accepted 3 February 2012

Available online 13 February 2012

Keywords:

Matrix metalloproteinases

Gelatinase inhibitors

Solid phase synthesis

Pyroglutamate

Thioprolin

ABSTRACT

Among matrix metalloproteinases (MMPs), gelatinases MMP-2 (gelatinase A) and MMP-9 (gelatinase B) play a key role in a number of physiological processes such as tissue repair and fibrosis. Many evidences point out their involvement in a series of pathological events, such as arthritis, multiple sclerosis, cardiovascular diseases, inflammatory processes and tumor progression by degradation of the extracellular matrix. To date, the identification of non-specific MMP inhibitors has made difficult the selective targeting of gelatinases. In this work we report the identification, design and synthesis of new gelatinase inhibitors with appropriate drug-like properties and good profile in terms of affinity and selectivity. By a detailed in silico protocol and innovative and versatile solid phase approaches, a series of 4-thiazolydinyl-*N*-hydroxycarboxamide derivatives were identified. In particular, compounds **9a** and **10a** showed a potent inhibitory activity against gelatinase B and good selectivity over the other MMP considered in this study. The identified compounds could represent novel potential candidates as therapeutic agents.

© 2012 Elsevier Ltd. All rights reserved.

1. Introduction

Matrix metalloproteinases (MMPs) are a family of approximately 27 zinc-dependent endopeptidases, involved in the proteolytic processing of several components of the extracellular matrix (ECM), such as collagen, proteoglycans and fibronectin.

In the last decades, considerable evidences have highlighted the involvement of abnormal MMP expression in several pathological conditions. In particular, MMP-2 and MMP-9, main enzymes able to degrade type IV collagen and gelatin, have been demonstrated to be directly involved in endothelial cell migration and vascular remodeling during angiogenesis, in tumor cell growth and progression during metastasis.

In the last twenty years, the blockage of the extracellular matrix degrading activities of MMPs has been considered an attractive strategy to treat a broad spectrum of diseases including cancer, neurological diseases, arthritis and cardiovascular pathologies.^{1–3} Moreover, although several potent MMPis have been discovered,^{4–8} the serious dose-limiting side effects occurring in clinical trials,^{9–11} probably due to the non-selective inhibitory activity, have underlined the importance to identify novel inhibitors able to discriminate among MMPs.^{12,13} In this scenario, the selective

inhibition of gelatinases may provide confidence for a successful clinical trial, targeting acute cardiovascular diseases and tumor progression.^{14–16} In particular MMP-2 is considered to be a better candidate target for anticancer drugs than MMP-9, whose inhibition is related to greater drug side effects.^{17,18}

In this paper we describe the identification of novel and selective gelatinase inhibitors by an in silico rational drug design approach and a versatile solid phase synthetic strategy. Starting from the MMP-2 complexes available in the Protein Data Bank (PDB),¹⁹ an active site mapping of gelatinase A was performed to generate the pharmacophore model used for the in silico screening of our in-house small molecule database. The screening was then followed by rational compound selection based on criteria, such as physico-chemical properties, ADMET predictions and synthetic feasibility. The computational approach led to the identification of the pyroglutamic moiety (Fig. 1) as a promising scaffold for the design and optimization of novel gelatinase inhibitors. By rational structure optimization, 4-thiazolydinyl-*N*-hydroxycarboxamide

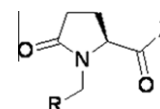


Figure 1. The pyroglutamic scaffold.

* Corresponding author. Tel.: +39 0672594029; fax: +39 0672594031.

E-mail address: alessandra.topai@uniroma2.it (A. Topai).

derivatives were identified as novel potential class of gelatinase inhibitors.

2. Results and discussion

2.1. MMP-2 binding site mapping and pharmacophore generation

The design of new gelatinase inhibitors started with the recognition of the representative examples of gelatinase complexes in the PDB. Focusing on MMP-2 structures in complex with inhibitors of known potency, the 11 NMR solution structures of MMP-2 catalytic domain (cd) (pdb code: 1hov) complexed with SC-74020 (MMP-2 IC_{50} less than 0.1 nM) and the crystal structure of cdMMP-2 (pdb code: 1qib) were selected for this work.

Overlay studies were carried out in order to identify inhibitor key features, required for protein recognition and thus significant for the pharmacophore model generation. The alignment, performed with a combinatorial extension (CE) algorithm,²⁰ showed a good overlay between the 11 NMR complexes and X-ray structure (RMSD in the range of 1.6–1.9 Å (Fig. 2a). Moreover, no significant difference in the binding mode of SC-74020, retrieved from the NMR complex with the lower RMSD with respect to 1qib structure (structure No. 7), was observed when the ligand was docked into the catalytic site of MMP-2 X-ray structure. As shown in Figure 2b, the hydroxamate zinc binding group (ZBG) is coordinated to Zn^{2+} ion, together with the catalytic histidine, while the P_1' group is involved in hydrophobic interactions with the amino acids of S_1' subsite, comprising a structurally stable hydrophobic pocket able to bind drug molecules at that position. According to the observed results, the more accurate MMP-2 X-ray structure was selected for further docking simulations.

By using MOE package software²¹ (see Section 5 for details), the selected SC-74020 NMR conformation was used to develop a pharmacophore model to mine novel and potential gelatinase inhibitors from our in-house virtual database, named MoDa. As shown in Figure 3, we considered two key pharmacophoric features: the ZBG and the P_1' moiety, which represent the two known binding and stabilizing interactions with the molecular target. In order to identify new scaffolds to be used for further investigations and

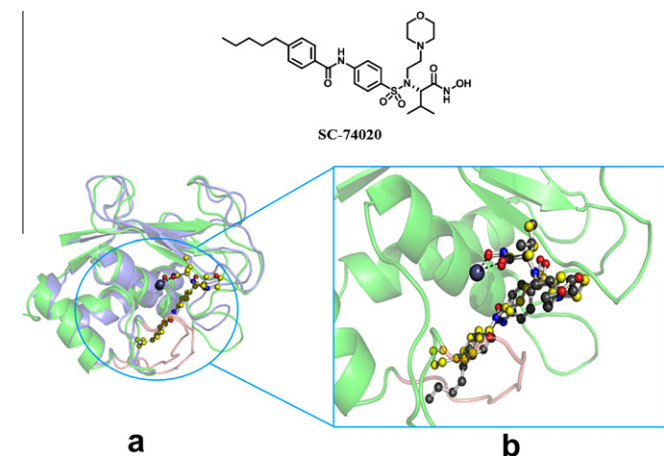


Figure 2. (a) Superimposition of NMR complex and X-ray MMP-2 structures, represented by blue and green cartoons, respectively. S_1' pocket is shown in pink while zinc ion is rendered as a light-gray sphere. The figure shows the NMR solution (No. 7 of 1hov.pdb) with lower RMSD compared to the MMP-2 X-ray coordinates, with SC-74020 rendered in yellow ball and stick figures. (b) Docking result of SC-74020 into the binding site of MMP-2 X-ray: the best scored pose and the NMR conformation are labeled as gray and yellow ball and stick figures, respectively.

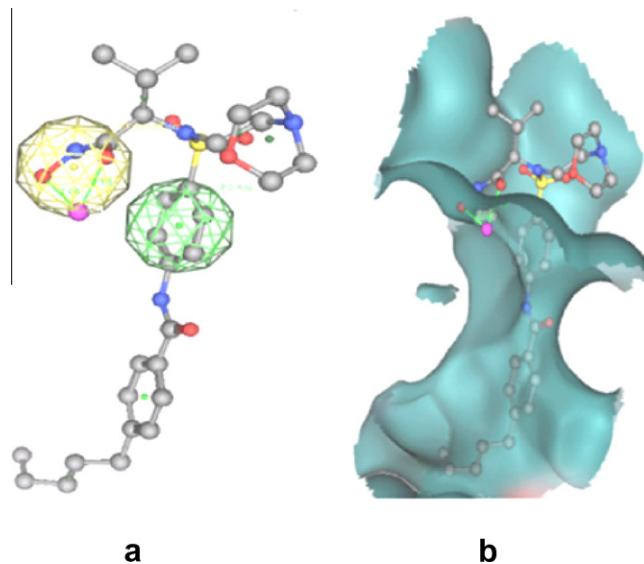


Figure 3. (a) Key pharmacophoric features defined on SC-74020 NMR conformation (pdb code: 1hov): F1 identified the zinc binding group, and the F2 corresponded to the P_1' aromatic ring group, labeled as yellow and green spheres, respectively. (b) The excluded volume defined by the protein residues with at least one atom within 4.5 Å from any atom of SC-74020.

deeper modifications, no further features were included to describe the long P_1' group.

2.2. 2D- and 3D-database generation

About 2 million unique commercially available small molecules have been collected in a proprietary 2D small molecule database, namely MoDa (Molecular Database). By using MOE, drug-like filters were applied to remove non drug-like, toxic or reactive molecules.^{22–24} Finally a number of around 600,000 unique structures were selected and for each molecule the 3D coordinates were derived. After energy minimization, for each 3D structure, a set of representative conformers was generated by molecular dynamic simulations. Low-energy conformations (≤ 5 kcal/mol from the global minimum) were included in the conformer database with a limit of 70 conformers per molecule, for the most flexible structures.

2.3. Pharmacophore based virtual screening

The derived 3D database was screened in MOE against the pharmacophore model. Hit compounds were ranked according to the score value defined by the RMSD of the aligned pharmacophoric points onto the pharmacophore model: no overlap on the excluded volume was permitted and, finally, about 200,000 molecules were identified. In order to select a more restricted number of compounds to be assayed against gelatinases, the selection was limited to a set of compounds bearing classical zinc binding groups (ZBG) such as carboxylic and hydroxamic acids. A molecular weight limit of 300 Da was imposed and a set of 150 compounds was obtained. Virtual hits were then visually inspected and selected following two criteria: synthetic feasibility and easiness to perform chemical modifications. Among the hit list, 15 compounds were selected, purchased, and assayed. The virtual screening flowchart is summarized in Figure 4, while the most representative compounds are depicted in Figure 5.

Among the screened compounds, the pyroglutamic acid derivative (*S*)-**1b** showed an in vitro MMP-2 inhibitory activity in the micromolar range ($IC_{50} = 315 \mu M$), prompting us to consider it

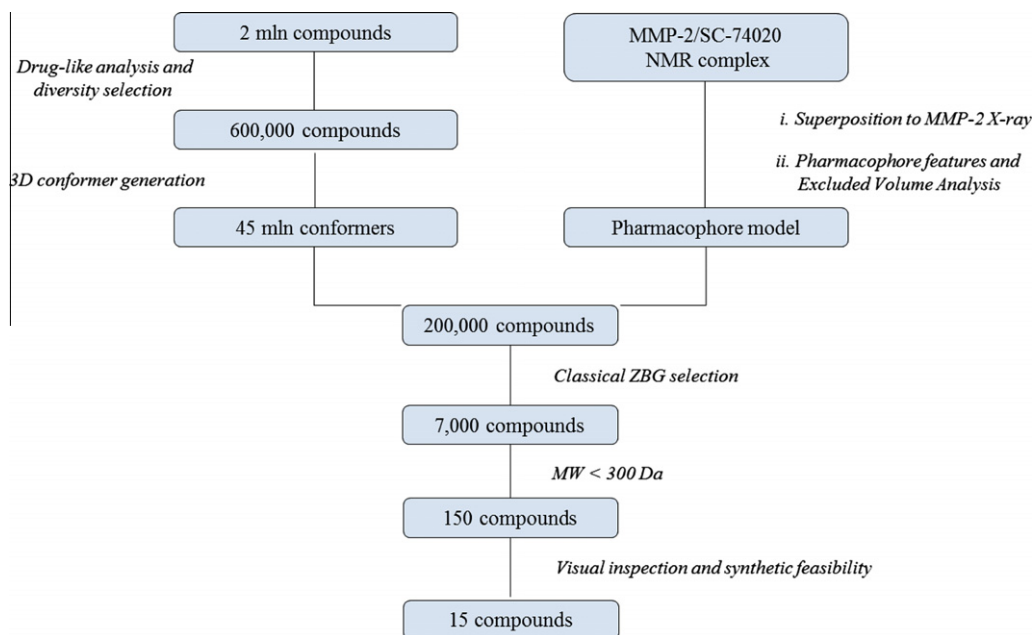


Figure 4. Virtual screening pharmacophore based flow-chart.

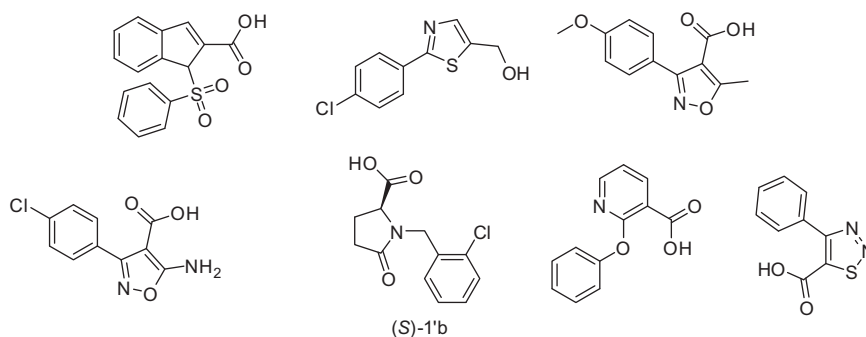


Figure 5. Selected hits from the in silico screening of MoDa database.

as a promising chemical scaffold for a new class of gelatinase inhibitors.

2.4. Chemical modification on selected scaffold

A first series of chemical modifications were performed on (S)-**1'b** template in order to investigate the influence on gelatinase inhibitory activity of (1) halogen position on the aromatic ring, (2) benzene ring replacement with a well-fitting P_1' substituent (biphenyl moiety), (3) introduction of a non-carboxylic acid ZBG (hydroxamic acid or amide group) and (4) chirality. These compounds were synthesized according to Schemes 1 and 2 and biologically screened against MMP-2 and MMP-9 (Table 1).

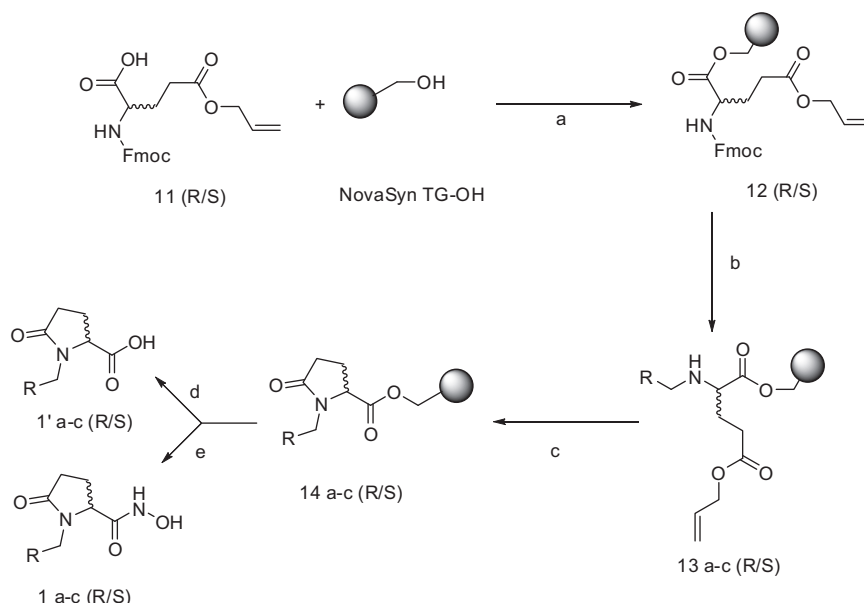
The biological data confirmed the expected results in terms of best ZBG and P_1' residues, while no significant effect of stereochemistry at C5 position was recorded. The in vitro screening led us to the identification of several hits and one of which, (S)-**1a**, was selected as the most versatile and promising hit, with a IC_{50} equal to 9 and 144 μ M on MMP-2 and MMP-9, respectively.

2.5. Hit to lead

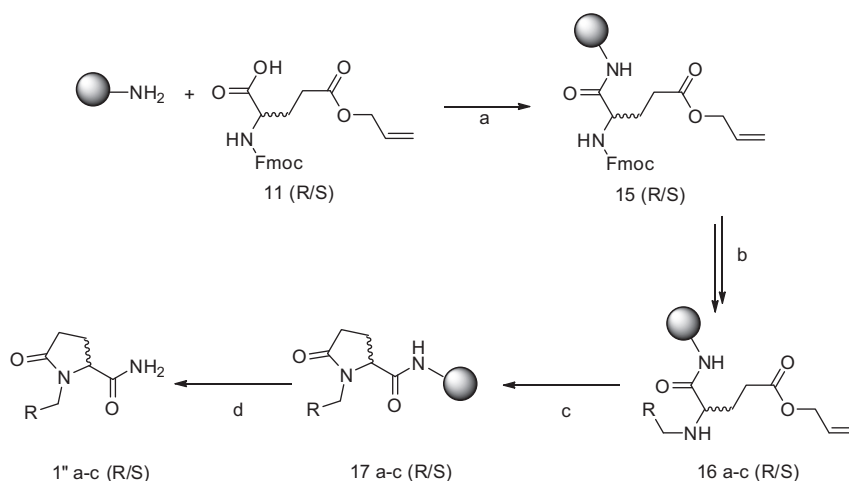
In order to improve gelatinase inhibitor potency, different chemical modifications were performed on the (S)-**1a** pyroglutamate

moiety, keeping the ZBG and P_1' groups unchanged (Fig. 6) and evaluating chemical modifications on the five-membered ring and the methylene group. The pyroglutamate ring was replaced with commercially available proline (**2a**), thiazolidine (**3a**) and hydroxyproline (**4a**). Thiazolidinone derivative **5a** was synthesized to investigate the influence of both the carbonyl group and the sulfur atom on the ring. Moreover, we synthesized the sulfonamide derivatives of pyroglutamate (**6a**), proline (**7a**), and thiazolidine (**8a**) since several literature data reported aryl-sulfonamide substituents to be the most favorable ones.²⁵

All novel compounds were synthesized (Scheme 3–6) and tested against gelatinases (Table 2). SAR analysis suggested that the introduction of a polar group, such as a carbonyl moiety at Y, maintaining a methylene group at Z position, strongly increases the inhibitory potency (i.e., **1a** vs **2a**; **5a** vs **3a**). Nevertheless, when the methylene group in Z is replaced with the SO_2 function, the influence of the carbonyl moiety in Y is negligible (i.e., **6a** vs **7a**). In contrast, the SO_2 group in Z enhances the positive effect of the substitution in the X position with a sulfur atom (compare compounds **2a/3a**, **1a/5a** and **7a/8a**). We identified compound **8a** as lead compound, with an IC_{50} value of 200 nM and of 230 nM towards MMP-2 and MMP-9, respectively. In order to get a more detailed representation of the recognition features, the compound was docked into the binding site of MMP-2 crystal structure.



Scheme 1. Reagents and conditions: (a) (1) DIC, dry DCM, rt, 1 h; (2) DMAP, dry DMF, rt, 2 h; (b) (1) 20% piperidine in DMF, 20 min, rt; (2) R-CHO, CH₃COOH, NaCNBH₃, in TMOF/MeOH, rt, 1 h; (c) (1) PhSiH₃, Pd[P(Ph)₃]₄, dry DCM (2 × 5 min); (2) HATU, DIEA, dry DMF, rt, 3 h; (d) NaOH 0.5%, rt, 1.5 h; (e) NH₂OH 50% wt in H₂O, THF, rt, 5 h.



Scheme 2. Reagents and conditions: (a) HBTU, HOBT, NMM, dry DMF, rt, 2 h; (b) (1) 20% piperidine in DMF, 20 min, rt; (2) R-CHO, CH₃COOH, NaCNBH₃, in TMOF/MeOH, rt, 1 h; (c) (1) PhSiH₃, Pd[P(Ph)₃]₄, dry DCM (2 × 5 min); (2) HATU, DIEA, dry DMF, rt, 3 h; (d) TFA/TIS (95:5), rt, 1 h.

The results revealed that compound **8a** adopts the expected binding mode with P₁' moiety involved in hydrophobic interactions with S₁' residues, giving high docking score in according with experimental data (data not shown).

2.6. **8a** scaffold optimization

From compound **8a** further modifications were performed on P₁' group. Several **8a** analogues bearing different bulky groups in R position were synthesized, most of them being related to known and potent MMP inhibitors. Furthermore, the effects on the biological activity of the –S– substitution on the five-membered ring with sulfoxide and sulfone moiety were evaluated.

All the compounds were synthesized and tested against MMP-2 and MMP-9 (Table 3). According to the biological data, the substitution of the biphenyl moiety with more rigid groups, such as naphthalene or quinoline, dramatically decreases the inhibitor

activity on both gelatinases (i.e., **8h** and **8i**), while, as expected, a relevant 20-fold improvement occurs upon substitution of the biphenyl ring with a *para*-substituted diaryl ether (see compounds **8j**, **8k**, **8l** in Table 3).

Subsequently, the accomplishment of a further improvement in inhibitory activity and a good degree of selectivity between the two gelatinases were achieved through substitution of –S– by –S(O)_n– (where *n* = 1 or 2, see compound **9a** and **10a** in Table 3).

To underline the selectivity profiles over other MMPs, the most promising compounds were tested against a broader panel of MMPs (Table 4).

Compounds **8k** and **8l** exhibited a relevant rate of discrimination with respect to MMP-1 and MMP-3. Moreover, compounds **9a** and **10a** showed a significant MMP-2 selectivity even over MMP-9. Unfortunately, more the activity increases, more the selectivity fades out. In addition, data collected for compound **10k** (Table 4) show that when gelatinase activity is in the low nanomol-

Table 1
Gelatinase A and B inhibitory activity of (R)- and (S)-1 derivatives

R	X	Cpd	IC ₅₀ (M) ^a		Cpd	IC ₅₀ (M) ^a	
			MMP-2 ^b	MMP-9 ^b		MMP-2 ^b	MMP-9 ^b
	CONHOH	(R)-1a	3 ± 0.3	30 ± 3	(S)-1a	9 ± 1	144 ± 10
	COOH	(R)-1'a	290	ND	(S)-1'a	340	ND
	CONH ₂	(R)-1''a	>500	ND	(S)-1''a	>500	ND
	CONHOH	(R)-1b	>500	>500	(S)-1b	>500	ND
	COOH	(R)-1'b	>500	ND	(S)-1'b	315	ND
	CONH ₂	(R)-1''b	>500	ND	(S)-1''b	>500	ND
	CONHOH	(R)-1c	400 ± 20	430	(S)-1c	>500	ND
	COOH	(R)-1'c	>500	ND	(S)-1'c	383	ND
	CONH ₂	(R)-1''c	>500	ND	(S)-1''c	>500	ND

^a ND: not determined.

^b MMP2: full length; MMP9: catalytic domain.

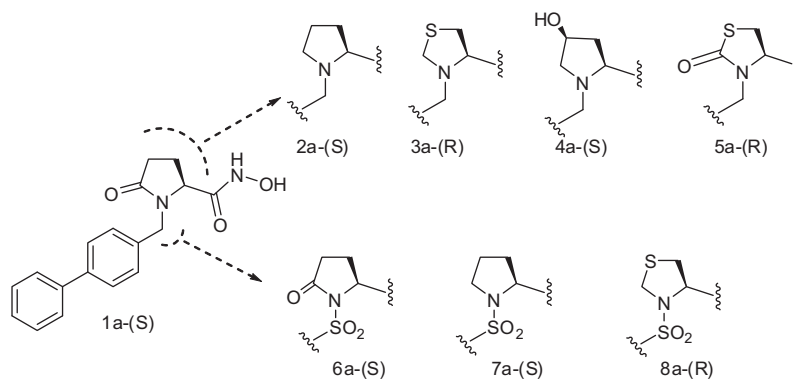


Figure 6. (S)-1a scaffold modifications.

lar range, high activity is recorded also towards other MMP members.

2.7. In silico investigation of MMP-2 selectivity over MMP-9

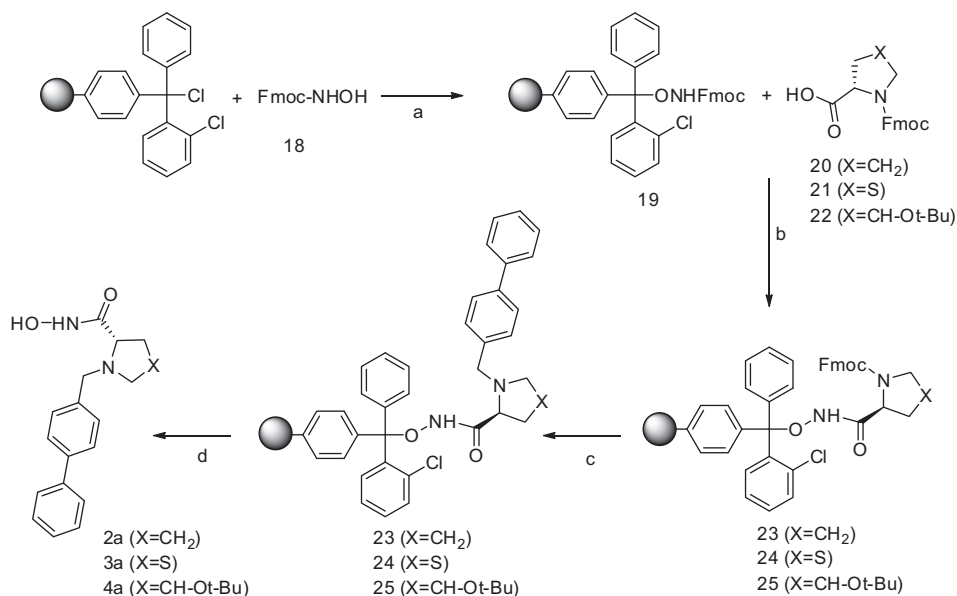
To investigate the different activity of **9a** and **10a** towards the two gelatinases, docking analysis on MMP-9 and MMP-2 binding sites was performed (see Section 5 for details). The comparison of the best scored solutions of both molecules highlighted a different binding mode in the two protein binding sites. For instance, visual inspection of **10a** binding mode (Fig. 7) revealed that one oxygen atom of the sulfonamide group can form an hydrogen bond with the NH group of MMP-9 Gln402 side-chain while in MMP-2 the hydroxamic NH group is involved in a hydrogen bond with the backbone of Ala165. The most remarkable difference in the binding modes of the two inhibitors relies on a significant change of overall shapes of the two heterocyclic rings in the two gelatinases. In MMP-2 binding site, one oxygen of the endocyclic SO₂/SO is involved in an hydrogen bond with the NH group of Ala164 backbone, while in MMP-9 the same group does not give further interactions, leading to a lower docking score (**10a**: 82.01 and 69.70,

respectively). The lack of this additional favorable interaction is probably due to the presence of a larger S₁' pocket that forces the molecules to plunge in deeply.

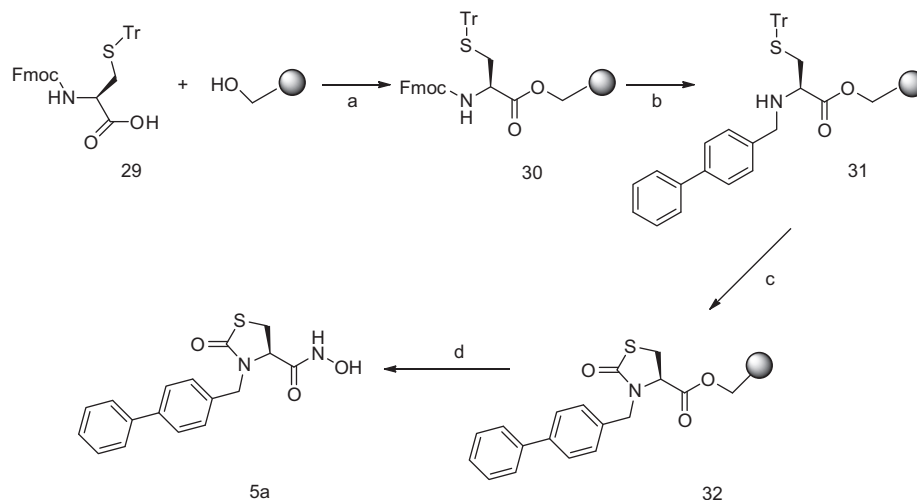
3. Solid phase synthesis

A versatile solid phase strategy for the synthesis of scaffolds 1–8 was developed.

In order to obtain compounds **1–1'–1''a–c** we performed a new synthetic solid phase approach using either a NovaSyn Tentagel resin or a Rink amide resin depending on whether the final cleavage should release a carboxylic/hydroxamic or an amidic moiety (Scheme 1 and 2). Both enantiomers of Fmoc-protected amino acid **11** were commercially available in pure enantiomeric form. Attachment to the resin followed by deprotection of the Fmoc group and subsequent reductive amination with appropriate alkylating reagents provided N-alkylated compounds **13–16a–c**. Removal of the protective group easily allowed condensation of the pyroglutamic ring to obtain **14–17a–c**. Final cleavage from the resin gave compounds **1–1'–1''a–c** with good purity degree (>90% by HPLC–MS).



Scheme 3. Reagents and conditions: (a) DIPEA, DCM, rt, 60 h; (b) (1) 20% piperidine in DMF, 20 min, rt; (2) HATU, DIPEA, DMF/DCM (1:1), rt, 12 h; (c) (1) 20% piperidine in DMF, 20 min, rt; (2) 4'-(Ph)-PhCHO, CH₃COOH, NaCNBH₃, in TMOF/MeOH, rt, 1 h; (d) AcOH/TFE/DCM (1:1:8), rt, 1 h.



Scheme 4. Reagents and conditions: (a) HATU, DIEA, DMAP, dry DMF/DCM, rt, 6 h; (b) (1) 20% piperidine in DMF, 20 min, rt; (2) R-CHO, CH₃COOH, NaCNBH₃, in TMOF/MeOH, rt, 1 h; (c) (1) TFA/TIS/DCM (10:5:85); (2) 10% Et₃N in DMF, 5 min, rt; (3) CDI, dry DCM, rt, 6 h; (d) NH₂OH 50% wt in H₂O, THF, rt, 5 h.

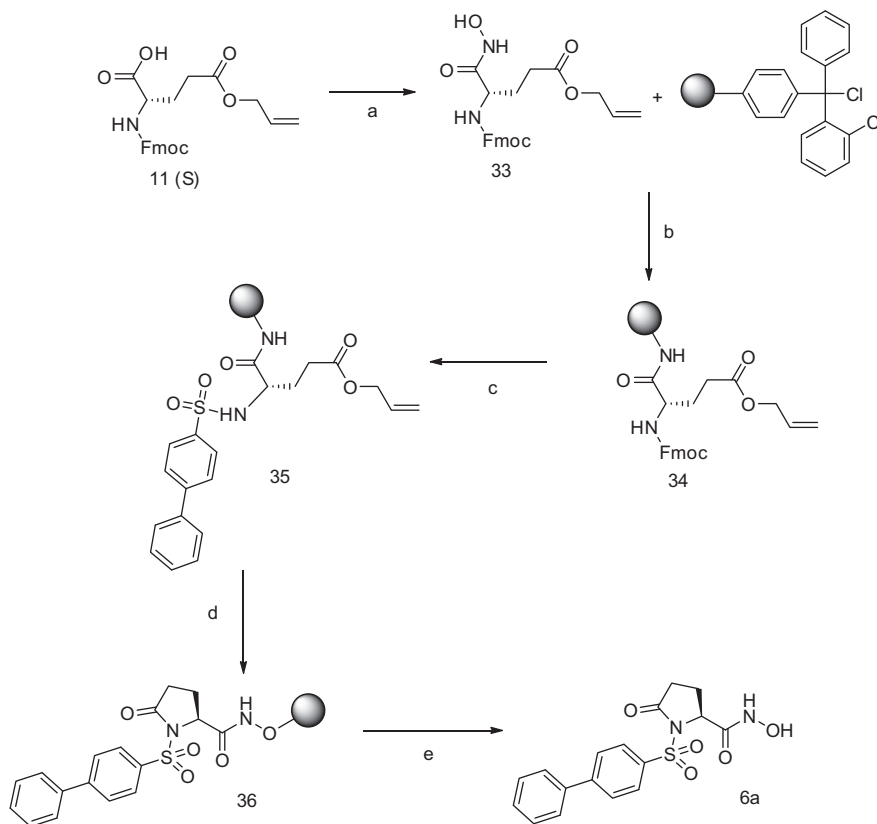
To obtain compounds **2a**, **3a** and **4a** Fmoc protected hydroxylamine was tethered to 2-chloro-chlorotrytil resin, which proved to be suitable to ensure the final release of hydroxamic derivatives (Scheme 3). After removal of the Fmoc group, coupling of compound **19** with Fmoc-protected proline/thioproline/hydroxyproline-carboxylic acids **20–22** gave compounds **23–25**. Fmoc group was then cleaved and subsequent reductive amination with *p*-phenylbenzaldehyde and cleavage from the resin released **2a**, **3a** and **4a** in good yields.

An innovative strategy was developed to obtain the oxothiazolidine hydroxamate derivative **5a** (Scheme 4). The compound was conveniently synthesized starting from Fmoc protected (*R*)-2-amino-3-(tritylthio)propanoic acid **29**. The substrate was anchored on NovaSyn Tentagel resin and after Fmoc cleavage reductive amination with *p*-phenylbenzaldehyde was performed. Compound **31** was then deprotected, cyclized, and cleaved from the resin to give compound **5a**.

An original pattern was then envisaged to synthesize compound **6**, which maintained the same ZBG and P₁ substituent as **5a**, changing the thiazolidinone ring into a pyrrolidinone (Scheme 5). Carboxylic acid (*S*)-**11** was converted to hydroxamic acid (*S*)-**33** and anchored on 2-chloro-chlorotrytil resin to obtain (*S*)-**34**. Then, Fmoc deprotection followed by sulfonamide synthesis gave (*S*)-**35**. Ring closing reaction occurred using the same conditions applied to synthesize derivatives **13** and **16** after acid deprotection (Scheme 1 and 2). Final cleavage from the resin using TFA produced **6** with high purity.

Compounds **7a**, **8a**, **8h–l**, **9a**, **10a**, **10k** were obtained only from two building blocks **20** and **21** (Scheme 6). NovaSyn Tentagel resin was chosen to tether the two acids. After Fmoc cleavage the amino group was reacted with several sulfonyl chlorides to obtain sulfonamides **39a** and **40a, h–l**.

Compounds **39a** and **40h–l** were immediately released from the resin to give **7a** and **8h–l**, while **40a** was split into two different



Scheme 5. Reagents and conditions: (a) (1) SOCl_2 , dioxane, 50°C , 2.5 h; (2) NH_2OH , DIEA, dioxane/ H_2O , rt, o.n. (b) (1) DIEA, DMF/DCM (1:10) rt, 60 h; (2) DCM/MeOH/DIEA (17:2:1), rt, 3×15 min; (c) (1) 20% piperidine in DMF, 20 min, rt; (2) DIEA, R-SO₂Cl, dry DCM, rt, o.n.; (d) (1) PhSiH_3 , $\text{Pd}[\text{P}(\text{Ph})_3]_4$, dry DCM (2×5 min); (2) HATU, DIEA, dry DMF, rt, 3 h; (e) TFA 5%, DCM, rt, 2 h.

batches. The first batch was used to give **8a**, the second one was oxidized with MCPBA, so to introduce a sulfone moiety on the ring to give **41a**. Compound **41a** was again split in two in order to obtain **9a** and perform the oxidation of sulfone to sulfoxide to finally release **10a**.

4. Conclusion

In conclusion, a pharmacophore based virtual screening of our in-house database and further chemical optimization led us to design novel gelatinase inhibitors. The compounds were synthesized developing and applying a solid phase approach. Docking simulations were performed to study the possible motifs of selectivity between MMP-2 and MMP-9. Notably, a very interesting selectivity was observed for some compounds with good in silico drug-like-ness profile. In particular the 4-thiazolydinyl-*N*-hydroxycarboxamide derivatives **9a** and **10a** showed a MMP-2 inhibitory activity in the low nanomolar range and a good selectivity over the MMPs analysed in this study. The achieved results represent a good starting point for future research activities, directed toward further medicinal chemistry optimizations.

5. Experimental section

5.1. Molecular modeling

5.1.1. MoDa-2D database

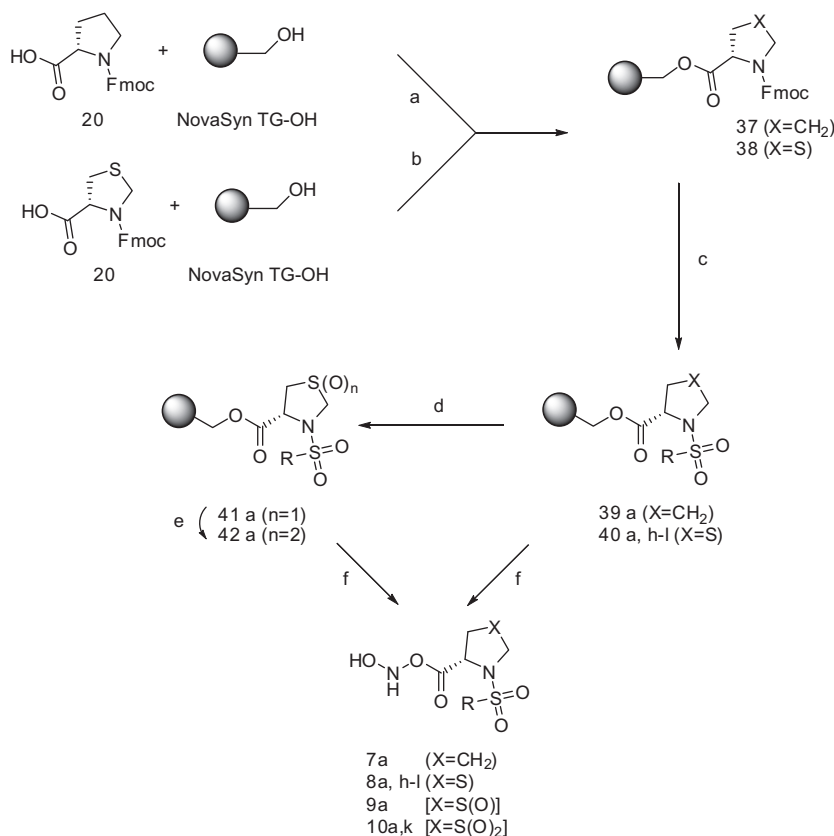
MoDa is a web-based application developed using the Perl programming language, containing about 2 millions distinct molecules from about 9 millions commercially available compounds. MoDa uses MySQL as Relational Database management System and Apache as web server.

5.1.2. MoDa-3D database

By using MOE, the compounds were selected from the MoDa-2D database according to the drug-like criteria, by property descriptor calculation, which include: number of violations of the Lipinsky's rule of five and other drug-like filters such as number of rings, number of halogens and undesirable reactive groups. A subset of about 600,000 compounds were selected and used to generate a database of conformers. The conformational analysis search was carried out via molecular dynamic (MD) as implemented in the MOE software package. For each compound, an MD run of 1 ns was performed using the NVT ensemble with $T = 300$ K, time step of 0.002 ps using MMFF94 force field and the Born solvation model. A total of 1000 conformations were collected for each MD run and they were energy-minimized requiring a RMSD of the gradient less than 0.05 kcal/mol.

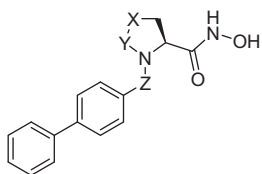
5.1.3. Pharmacophore design

MOE Pharmacophore Applications module has been used to design pharmacophore hypotheses and to perform database screening. The PCH pharmacophore scheme included the following atomic tags: H-Bond Acceptor, H-Bond Donor, Cation, Anion, Aromatic ring center, Hydrophobic Region, Metal Ligator, Volume Constraint. In detail, by using SC-74020 ligand coordinates as reference template, the first pharmacophoric point was fixed on hydroxamic group setting a tolerance radius of 1.8 Å to include one or both oxygen atoms of alternative other ZBGs (e.g. carboxylic acids, hydroxamic acids, phosphates). The second pharmacophoric point was defined on the P_1' phenyl group, with a tolerance radius comparable with the size of an aromatic ring (1.8 Å). Finally, the overall shape of the protein around the catalytic site and the S_1' pocket was modeled considering the excluded volume defined by the protein residues with at least one atom within 4.5 Å from any atom



Scheme 6. Reagents and conditions: (a) HATU, DIPEA, dry DCM/DMF (1:1), rt, 12 h; (b) DMAP, dry DMF, rt, 12 h; (c) (1) 20% piperidine in DMF, 20 min, rt; (2) DMAP, R-SO₂-Cl, THF/DCM (2:1) rt, 12 h; (d) MCPBA, dry DCM, rt, 27 h; (e) MCPBA, dry DCM, rt, 27 h; (f) NH₂OH 50% wt in H₂O, THF, rt, 5 h.

Table 2
Gelatinase A and B inhibitory activity of **1–8a** compounds



Compd	X	Y	Z	IC ₅₀ (μM)	
				MMP2wh ^a	MMP9cd ^b
1a	CH ₂	C(O)	CH ₂	9 ± 1	144 ± 10
2a	CH ₂	CH ₂	CH ₂	>500	ND
3a	S	CH ₂	CH ₂	330 ± 15	ND
4a	CH(OH)	CH ₂	CH ₂	>500	ND
5a	S	C(O)	CH ₂	6.80 ± 1	47 ± 8
6a	CH ₂	C(O)	SO ₂	1.7 ± 0.5	1.9 ± 0.1
7a	CH ₂	CH ₂	SO ₂	4 ± 1	76 ± 4
8a	S	CH ₂	SO ₂	0.20 ± 0.01	0.23 ± 0.05

^a MMP2wh: MMP2 full length.

^b MMP9: full length; MMP9: catalytic domain.

of SC-74020. Around 200 atom points were used to describe the excluded volume in such a manner that also larger inhibitors should satisfy the same query (Fig. 3b).

5.1.4. Docking simulations

In the present study, the 3D coordinates of MMP-2 and MMP-9 (pdb codes: 1qib and 2ow1, respectively) were retrieved from the PDB. Protein preparation was performed in MOE: the two proteins

were aligned, the water molecules, cofactors and (MMP-9) co-crystallized ligand were removed; by using Protonate 3D tool, the hydrogen atoms were added, fixing the correct protonation of protein residues. The inhibitors described in this work were built from the MOE fragment library and minimized by setting MMFF94 force field.

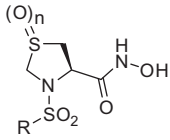
Docking simulations were performed using the GOLD program (Cambridge Crystallographic Data Centre, Cambridge, UK) by setting the GoldScore (GS) fitness functions to quantify the interaction energy of ligand–protein complexes. The fitness function parameters were taken from the GOLD parameter file. The binding cavities contained the protein residues in a sphere of a 12 Å radius centred on the SC-74020 aromatic carbon C18. Zinc trigonal/bipyramidal coordination geometry was imposed. For each compounds, 10 poses were generated into the binding site of MMP-2 and MMP-9, respectively. The binding mode inspections were carried out by Hermes Viewer implemented in GOLD software.

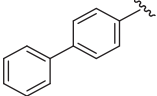
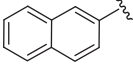
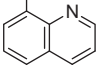
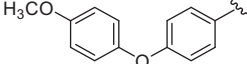
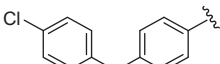
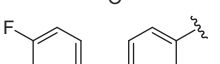
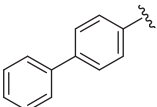
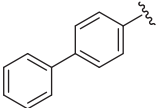
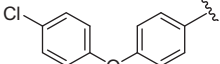
5.1.5. Additional softwares

Visual inspections of docking and pharmacophore analysis were performed with PyMOL.²⁶ In addition MOE, Babel, CDK and JOELib were used as chemoinformatic tools for SMARTS search, conversion, and other routine tasks.

5.2. Chemistry

Reagents and solvents were obtained from commercial suppliers and used without further purification. Thin layer chromatography (TLC) analytical separations were conducted with E. Merck Silica Gel F-254 plates of 0.25 mm thickness and were visualized with UV light (254 nm) or I₂. Flash chromatography was performed

Table 3
MMP-2 e MMP-9 screening results of 8a analogues


Compd	n	R	IC ₅₀ (nM)	
			MMP2wh	MMP9cd
8a	0		200 ± 10	230 ± 50
8h	0		31,000 ± 500	>50,000
8i	0		710 ± 40	560 ± 30
8j	0		9 ± 1	2 ± 0.3
8k	0		13 ± 5	16 ± 9
8l	0		10 ± 2	5 ± 0.5
9a	1		9 ± 3	600 ± 100
10a	2		53 ± 16	480 ± 80
10k	2		0.8 ± 0.1	0.5 ± 0.07

using E. Merck silica gel. ¹H nuclear magnetic resonance (NMR) spectra were recorded in the specified deuterated solvents on a Bruker Avance 300 spectrometer operating at 300 MHz. Chemical shifts are reported in parts per million (δ) from the tetramethylsilane resonance in the indicated solvent (TMS: 0.0 ppm). Compounds purities and mass spectra were determined by an LC/MS platform (Gilson/ThermoFinnigan) using the positive electrospray ionization technique (+ES) with a mobile phase of acetonitrile/water with 0.1% TFA.

Table 4
Biological data collected for compounds 8a analogues

Compd	IC ₅₀ (nM)						
	MMP2	MMP9	MMP1cd	MMP3cd	MMP8cd	MMP12cd	MMP14cd
8j	9 ± 1	2 ± 0.3	ND	ND	ND	ND	ND
8k	13 ± 5	16 ± 9	1000 ± 50	160 ± 30	ND	ND	ND
8l	10 ± 2	5 ± 0.5	>50,000	700 ± 100	ND	ND	ND
9a	9 ± 3	600 ± 100	4000 ± 500	2000 ± 300	400 ± 100	2500 ± 500	160 ± 20
10a	53 ± 16	480 ± 80	2500 ± 100	4000 ± 100	100 ± 40	500 ± 10	3800 ± 500
10k	0.8 ± 0.1	0.5 ± 0.07	ND	ND	4 ± 1	19 ± 6	5 ± 0.5

Elementary analyses were performed on a Perkin-Elmer 2400 Series II Elemental Analyser and a microbalance AD-4 autobalance Perkin-Elmer.

Optical rotations were determined at 25 °C on a Perkin-Elmer 341 polarimeter (concentrations are reported in units of grams per 100 mL).

5.2.1. General methods for solid phase synthesis

Solvents were distilled for resin reactions. Unless otherwise stated reactions were performed in 8 mL polypropylene cartridges with 70 mm PE frits. Cartridges and stopcocks were obtained from Applied Separations. All Fmoc amino acids, coupling reagents, and resins were purchased from Novabiochem, and other chemicals were from Aldrich.

5.2.2. General procedures for coupling of Fmoc-(D/L)-Glu-(OAll)-OH to NovaSynTGOH

Example: Synthesis of (R)-12.

N,N'-Diisopropylcarbodiimide (DIC) (300 μl, 1.9 mmol) was added to a solution of Fmoc-D-Glu-(OAll)-OH (**R**)-11 (1.55 g, 3.8 mmol) in 10 ml dry DCM at 0 °C. After stirring at room temperature for 1 h, DCM was evaporated, 3 ml of DMF were added and the solution was dropped into the cartridge in which hydroxyl group functionalized resin (NovaSynTGOH) (1.26 g, 0.38 mmol) was pre-swollen in DCM. 4-Dimethylaminopyridine (DMAP) (5 mg, 0.04 mmol) in 0.3 ml dry DMF was introduced and the cartridge was gently rocked for 2 h at room temperature.

After filtration the resin was rinsed with DMF (3 × 5 ml), DCM (3 × 5 ml) and TBME (3 × 5 ml) and finally dried in vacuo.

The efficiency of loading (loading yield: 81%) was determined on 5.9 mg of resin by Fmoc removal analysis (treatment of the resin with piperidine 20% in DMF) and absorbance measurement at 301 nm (UV-vis Spectrophotometer Shimadzu).

5.2.3. General procedures for Fmoc deprotection and reductive amination of polymer bound O-All-(D/L) glutamate

Example: Synthesis of (R)-13a.

After Fmoc deprotection with 20% piperidine in DMF for 20 min (×2), (**R**)-12 (0.08 mmol) was washed (2 × DMF, 2 × DCM) and swollen in DCM, then biphenyl-4-carboxaldehyde (120 mg, 0.66 mmol) in 0.8 ml trimethyl orthoformate (TMOF) was added dropwise. Subsequently methanol (MeOH) (200 μl), acetic acid (38 μl, 0.66 mmol) and NaCNBH₃ (124 mg, 1.97 mmol) in MeOH (400 μl) were respectively introduced into the reaction mixture. After shaking for 1 h at room temperature, the resin was filtered and washed with MeOH (×3), DMF (×3), DCM (×3) and TBME (×3).

5.2.4. General procedures for allyl deprotection and cyclization

Example: Synthesis of (R)-14a.

PhSiH₃ (500 μl, 4.1 mmol) and Pd[P(Ph)₃]₄ (95 mg, 0.08 mmol) in 2 ml dry DCM were added to 0.08 mmol of (**R**)-13a pre-swollen in DCM.

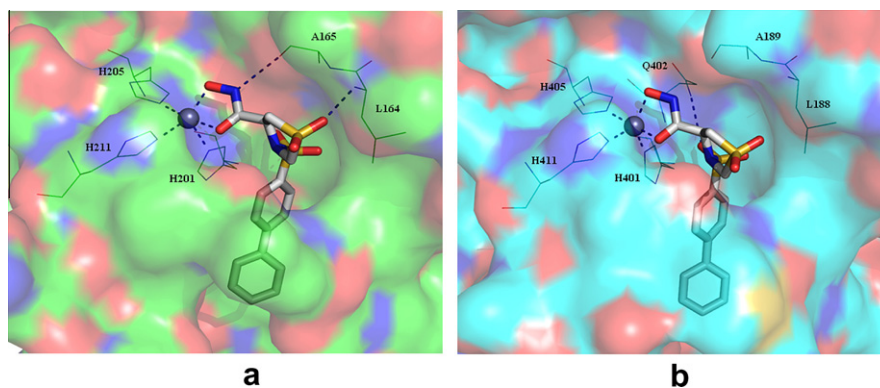


Figure 7. Docking results of compound **10a** into the binding site of MMP-2 (a) and MMP-9 (b). The proteins are rendered as green and cyan surfaces, respectively. The relevant residues are depicted as line figures. The most important interactions between ligand and protein residues and metal coordinations are rendered as blue dashed lines. Zinc ion is rendered as gray sphere.

After repeating the treatment twice (2×5 min) the resin was filtered, rinsed first with DCM, and later with a solution of DIEA (0.5%) and $\text{NaEt}_2\text{NCS}_2$ (0.5%) in DMF, and again with DMF, DCM and DMF.

DIEA (17 μl , 0.01 mmol) and a solution of HATU (2-(1*H*-9-azabenzotriazole-1-yl)-1,1,3,3-tetramethyluronium hexafluorophosphate) (38 mg, 0.01 mmol) previously dissolved in 0.7 ml of dry DMF were introduced into the cartridge; the cyclization proceeded for 3 h at room temperature. The resin was filtered and rinsed with DMF ($\times 3$), MeOH ($\times 3$), DCM ($\times 3$) and TBME ($\times 3$).

5.2.5. General procedures for the cleavage of hydroxamate derivatives 1

Example: (*R*)-1-(4-phenylbenzyl)-*N*-hydroxy-5-oxopyrrolidine-2-carboxamide [(*R*)-**1a**].

Functionalized resin derivative (*R*)-**14a** (0.04 mmol) was swollen in THF (1.8 ml) and cleaved from the solid support by treatment with 50% NH_2OH in H_2O (300 μl , 5.6 mmol). After rocking for 5 h at room temperature, the resin was filtered and the filtrate was evaporated to dryness.

The crude product was further purified by semi-preparative RP-HPLC (C18, Nucleosil 300 mm \times 25 mm, 3 ml/min, detection at 230 nm, eluent A: Water/TFA: 99.92:0.08, eluent B: acetonitrile/TFA: 99.92:0.08; gradient B from 20% to 80% in 14 min, from 80% to 98% in 3 min) to afford (*R*)-**1a**.

Amorphous solid— ^1H NMR (300 MHz, $\text{DMSO}-d_6$): δ 1.82–1.90 (m, 1H), 2.1–2.2 (m, 1H), 2.29–2.45 (m, 2H), 3.65 (d, 1H, $J = 14.7$ Hz), 3.82 (dd, 1H, $J = 8.8, 3.9$ Hz), 4.90 (d, 1H, $J = 14.7$ Hz), 7.27 (d, 2H, $J = 7.8$ Hz), 7.36 (t, 1H, $J = 14.7, 7.8$ Hz), 7.46 (dd as t, 2H, $J = 15.6, 7.8$ Hz), 7.63 (d, 2H, $J = 7.8$ Hz), 7.65 (d, 2H, $J = 5.9$ Hz), 9.08 (br s, 1H), 10.79 (br s, 1H). LC-MS (ESI) ($\text{H}_2\text{O}/\text{CH}_3\text{CN}$, 1%TFA) m/z (%): 311.3 (MH^+ , 100), $\text{C}_{18}\text{H}_{18}\text{N}_2\text{O}_3$: 310.3. Specific optical rotation $[\alpha]_{\text{D}}^{25} -51$ (c 0.02, CH_3OH). Anal. Calcd for $\text{C}_{18}\text{H}_{18}\text{N}_2\text{O}_3$: C, 69.66; H, 5.85; N, 9.03; O, 15.47. Found: C, 69.99; H, 5.83; N, 9.05; O, 15.23. Overall yield 12%.

5.2.5.1. (*S*)-**1a**: (*S*)-1-(4-Phenylbenzyl)-*N*-hydroxy-5-oxopyrrolidine-2-carboxamide.

Amorphous solid— ^1H NMR (300 MHz, $\text{DMSO}-d_6$): δ 1.83–1.88 (m, 1H), 2.11–2.21 (m, 1H), 2.29–2.46 (m, 2H), 3.65 (d, 1H, $J = 15.6$ Hz), 3.82 (dd, 1H, $J = 8.8, 3.9$ Hz), 4.91 (d, 1H, $J = 15.6$ Hz), 7.27 (d, 2H, $J = 7.8$ Hz), 7.36 (dd as t, 1H, $J = 14.7, 6.86$ Hz), 7.46 (dd as t, 2H, $J = 14.7, 6.86$ Hz), 7.63 (d, 2H, $J = 7.8$ Hz), 7.65 (d, 2H, $J = 5.9$ Hz), 9.08 (br s, 1H), 10.79 (br s, 1H). LC-MS (ESI) ($\text{H}_2\text{O}/\text{CH}_3\text{CN}$, 1%TFA) m/z (%): 311.2 (MH^+ , 100), $\text{C}_{18}\text{H}_{18}\text{N}_2\text{O}_3$: 310.3. Specific optical rotation $[\alpha]_{\text{D}}^{25} +53$ (c 0.02,

CH_3OH). Anal. Calcd for $\text{C}_{18}\text{H}_{18}\text{N}_2\text{O}_3$: C, 69.66; H, 5.85; N, 9.03; O, 15.47. Found: C, 69.93; H, 5.86; N, 9.04; O, 15.42. Overall yield 15%.

5.2.5.2. (*R*)-**1b**: (*R*)-1-(2-Chlorobenzyl)-*N*-hydroxy-5-oxopyrrolidine-2-carboxamide.

Amorphous solid— ^1H NMR (300 MHz, $\text{DMSO}-d_6$): δ 1.84–1.91 (m, 1H), 2.18–2.27 (m, 1H), 2.29–2.45 (m, 2H), 3.83–3.87 (m, 2H), 4.79 (d, 1H, $J = 15.6$ Hz), 7.21–7.23 (m, 1H), 7.32–7.34 (m, 2H), 7.45–7.47 (m, 1H), 9.07 (br s, 1H), 10.74 (br s, 1H). LC-MS (ESI) ($\text{H}_2\text{O}/\text{CH}_3\text{CN}$, 1%TFA) m/z (%): 269.1 (MH^+ , 100), $\text{C}_{12}\text{H}_{13}\text{ClN}_2\text{O}_3$: 268.7. Specific optical rotation $[\alpha]_{\text{D}}^{25} -68$ (c 0.09, CH_3OH). Anal. Calcd for $\text{C}_{12}\text{H}_{13}\text{ClN}_2\text{O}_3$: C, 53.64; H, 4.88; Cl, 13.19; N, 10.43; O, 17.86. Found: C, 53.44; H, 4.87; Cl, 13.15; N, 10.45; O, 17.90.

5.2.5.3. (*S*)-**1b**: (*S*)-1-(2-Chlorobenzyl)-*N*-hydroxy-5-oxopyrrolidine-2-carboxamide.

Amorphous solid— ^1H NMR (300 MHz, $\text{DMSO}-d_6$): δ 1.84–1.92 (m, 1H), 2.16–2.26 (m, 1H), 2.29–2.45 (m, 2H), 3.82–3.84 (m, 1H), 3.85 (d, 1H, $J = 15.6$ Hz), 4.79 (d, 1H, $J = 15.6$ Hz), 7.21–7.23 (m, 1H), 7.31–7.34 (m, 2H), 7.45–7.47 (m, 1H), 9.06 (br s, 1H), 10.75 (br s, 1H). LC-MS (ESI) ($\text{H}_2\text{O}/\text{CH}_3\text{CN}$, 1%TFA) m/z (%): 269.1 (MH^+ , 100), $\text{C}_{12}\text{H}_{13}\text{ClN}_2\text{O}_3$: 268.7. Specific optical rotation $[\alpha]_{\text{D}}^{25} +66$ (c 0.09, CH_3OH). Anal. Calcd for $\text{C}_{12}\text{H}_{13}\text{ClN}_2\text{O}_3$: C, 53.64; H, 4.88; Cl, 13.19; N, 10.43; O, 17.86. Found: C, 53.50; H, 4.87; Cl, 13.17; N, 10.45; O, 17.88. Overall yield 11%.

5.2.5.4. (*R*)-**1c**: (*R*)-1-(4-Chlorobenzyl)-*N*-hydroxy-5-oxopyrrolidine-2-carboxamide.

Amorphous solid— ^1H NMR (300 MHz, $\text{DMSO}-d_6$): δ 1.81–1.88 (m, 1H), 2.09–2.19 (m, 1H), 2.26–2.43 (m, 2H), 3.65 (d, 1H, $J = 15.6$ Hz), 3.76 (dd, 1H, $J = 7.8, 3.91$ Hz), 4.79 (d, 1H, $J = 15.6$ Hz), 7.21 (d, 2H, $J = 8.8$ Hz), 7.39 (d, 2H, $J = 8.8$ Hz), 9.08 (br s, 1H), 10.74 (br s, 1H). LC-MS (ESI) ($\text{H}_2\text{O}/\text{CH}_3\text{CN}$, 1%TFA) m/z (%): 269.1 (MH^+ , 100), $\text{C}_{12}\text{H}_{13}\text{ClN}_2\text{O}_3$: 268.7. Specific optical rotation $[\alpha]_{\text{D}}^{25} -55$ (c 0.04, CH_3OH). Anal. Calcd for $\text{C}_{12}\text{H}_{13}\text{ClN}_2\text{O}_3$: C, 53.64; H, 4.88; Cl, 13.19; N, 10.43; O, 17.86. Found: C, 53.58; H, 4.87; Cl, 13.16; N, 10.41; O, 17.82. Overall yield 13%.

5.2.5.5. (*S*)-**1c**: (*S*)-1-(4-Chlorobenzyl)-*N*-hydroxy-5-oxopyrrolidine-2-carboxamide.

Amorphous solid— ^1H NMR (300 MHz, $\text{DMSO}-d_6$): δ 1.81–1.89 (m, 1H), 2.07–2.17 (m, 1H), 2.25–2.41 (m, 2H), 3.65 (d, 1H, $J = 15.6$ Hz), 3.75 (dd, 1H, $J = 7.8, 3.9$ Hz), 4.78 (d, 1H, $J = 15.6$ Hz), 7.21 (d, 2H, $J = 8.8$ Hz), 7.39 (d, 2H, $J = 8.8$ Hz), 9.11 (br s, 1H), 10.82 (br s, 1H). LC-MS (ESI) ($\text{H}_2\text{O}/\text{CH}_3\text{CN}$, 1%TFA) m/z (%): 269.1 (MH^+ , 100), $\text{C}_{12}\text{H}_{13}\text{ClN}_2\text{O}_3$: 268.7. Specific optical rotation $[\alpha]_{\text{D}}^{25} +56$ (c 0.04, CH_3OH). Anal. Calcd for $\text{C}_{12}\text{H}_{13}\text{ClN}_2\text{O}_3$: C,

53.64; H, 4.88; Cl, 13.19; N, 10.43; O, 17.86. Found: C, 53.61; H, 4.87; Cl, 13.18; N, 10.41; O, 17.84. Overall yield 13%.

5.2.6. General procedures for the cleavage of carboxylate derivatives 1'

Example: (R)-1-(4-phenylbenzyl)-5-oxopyrrolidine-2-carboxylic acid [(R)-1'a].

Functionalized resin derivative (R)-14a (0.04 mmol) was swollen in THF (1.8 ml) and cleaved by NaOH 0.5% solution (2.5 ml, 0.37 mmol). After rocking for 1.5 h at room temperature, the resin was filtered and the filtrate was evaporated to dryness.

Deprotected (R)-1'a was purified by semi-preparative RP-HPLC (C18, Nucleosil 300 mm × 25 mm, 3 ml/min, detection at 230 nm, eluent A: Water/TFA: 99.92:0.08, eluent B: acetonitrile/TFA: 99.92:0.08; gradient B from 25% to 60% in 13 min, from 60% to 98 in 1 min).

Waxy solid—¹H NMR (300 MHz, DMSO-*d*₆): δ 1.93–2.0 (m, 1H), 2.26–2.38 (m, 3H), 3.93–3.98 (m, 2H), 4.91 (d, 1H, *J* = 14.9 Hz), 7.29 (d, 2H, *J* = 7.8 Hz), 7.36 (t, 1H, *J* = 7.4 Hz), 7.46 (t, 2H, *J* = 7.4 Hz), 7.63 (d, 2H, *J* = 8.2 Hz), 7.65 (d, 2H, *J* = 7.4 Hz). LC–MS (ESI) (H₂O/CH₃CN, 1%TFA) *m/z* (%): 296.2 (MH⁺, 100), C₁₈H₁₇NO₃: 295.3. Specific optical rotation [α]_D²⁵ –50 (c 0.01, CH₃OH). Anal. Calcd for C₁₈H₁₇NO₃: C, 73.20; H, 5.80; N, 4.74; O, 16.25. Found: C, 73.17; H, 5.79; N, 4.75; O, 16.26. Overall yield 15%.

5.2.6.1. (S)-1'a: (S)-1-(4-Phenylbenzyl)-N-hydroxy-5-oxopyrrolidine-2-carboxamide.

Waxy solid—¹H NMR (300 MHz, DMSO-*d*₆): δ 1.94–2.0 (m, 1H), 2.26–2.38 (m, 3H), 3.93–3.97 (m, 2H), 4.9 (d, 1H, *J* = 15.3 Hz), 7.29 (d, 2H, *J* = 8.2 Hz), 7.36 (t, 1H, *J* = 7.4 Hz), 7.46 (dd as t, 2H, *J* = 7.4 Hz), 7.63 (d, 2H, *J* = 8.2 Hz), 7.65 (d, 2H, *J* = 7.8 Hz). LC–MS (ESI) (H₂O/CH₃CN, 1%TFA) *m/z* (%): 296.2 (MH⁺, 100), C₁₈H₁₇NO₃: 295.3. Specific optical rotation [α]_D²⁵ +56 (c 0.05, CH₃OH). Anal. Calcd for C₁₈H₁₇NO₃: C, 73.20; H, 5.80; N, 4.74; O, 16.25. Found: C, 73.15; H, 5.81; N, 4.75; O, 16.28. Overall yield 17%.

5.2.6.2. (R)-1'b: (R)-1-(2-Chlorobenzyl)-5-oxopyrrolidine-2-carboxylic acid.

Waxy solid—¹H NMR (300 MHz, DMSO-*d*₆): δ 1.98 (m, 1H), 2.29–2.37 (m, 3H), 3.96 (d, 1H, *J* = 6.3 Hz), 4.11 (d, 1H, *J* = 15.6 Hz), 4.85 (d, 1H, *J* = 15.3 Hz), 7.24–7.26 (m, 1H), 7.31–7.35 (m, 2H), 7.44–7.48 (m, 1H). LC–MS (ESI) (H₂O/CH₃CN, 1%TFA) *m/z* (%): 254.1 (MH⁺, 98), C₁₂H₁₂ClNO₃: 253.7. Specific optical rotation [α]_D²⁵ –18 (c 0.07, CH₃OH). Anal. Calcd for C₁₂H₁₂ClNO₃: C, 56.81; H, 4.77; Cl, 13.98; N, 5.52; O, 18.92. Found: C, 56.94; H, 4.78; Cl, 13.99; N, 5.53; O, 18.96. Overall yield 18%.

5.2.6.3. (S)-1'b: (S)-1-(2-Chlorobenzyl)-5-oxopyrrolidine-2-carboxylic acid.

Waxy solid—¹H NMR (300 MHz, DMSO-*d*₆): δ 1.98 (m, 1H), 2.33 (m, 3H), 3.97 (d, 1H, *J* = 6.3 Hz), 4.11 (d, 1H, *J* = 15.6 Hz), 4.85 (d, 1H, *J* = 15.6 Hz), 7.25–7.28 (m, 1H), 7.31–7.35 (m, 2H), 7.44–7.48 (m, 1H). LC–MS (ESI) (H₂O/CH₃CN, 1%TFA) *m/z* (%): 254.1 (MH⁺, 100), C₁₂H₁₂ClNO₃: 253.7. Specific optical rotation [α]_D²⁵ +23 (c 0.1, CH₃OH). Anal. Calcd for C₁₂H₁₂ClNO₃: C, 56.81; H, 4.77; Cl, 13.98; N, 5.52; O, 18.92. Found: C, 56.88; H, 4.78; Cl, 13.97; N, 5.53; O, 18.94. Overall yield 15%.

5.2.6.4. (R)-1'c: (R)-1-(4-Chlorobenzyl)-5-oxopyrrolidine-2-carboxylic acid.

Waxy solid—¹H NMR (300 MHz, DMSO-*d*₆): δ 1.92–1.98 (m, 1H), 2.22–2.37 (m, 3H), 3.93–3.97 (m, 2H), 4.79 (d, 1H, *J* = 15.3 Hz), 7.23 (d, 2H, *J* = 8.6 Hz), 7.39 (d, 2H, *J* = 8.6 Hz). LC–MS (ESI) (H₂O/CH₃CN, 1%TFA) *m/z* (%): 254.1 (MH⁺, 75), C₁₂H₁₂ClNO₃: 253.7. Specific optical rotation [α]_D²⁵ –78 (c 0.03, CH₃OH). Anal. Calcd for C₁₂H₁₂ClNO₃: C, 56.81; H, 4.77; Cl, 13.98; N, 5.52; O, 18.92. Found: C, 56.65; H, 4.76; Cl, 13.94; N, 5.50; O, 18.87. Overall yield 15%.

5.2.6.5. (S)-1'c: (S)-1-(4-Chlorobenzyl)-5-oxopyrrolidine-2-carboxylic acid.

Waxy solid—¹H NMR (300 MHz, DMSO-*d*₆): δ 1.91–1.98 (m, 1H), 2.21–2.37 (m, 3H), 3.91 (d, 1H, *J* = 9.0 Hz), 3.95 (d, 1H, *J* = 15.3 Hz), 4.79 (d, 1H, *J* = 15.3 Hz), 7.23 (d, 2H, *J* = 8.2 Hz), 7.39 (d, 2H, *J* = 8.2 Hz). LC–MS (ESI) (H₂O/CH₃CN, 1%TFA) *m/z* (%): 254.1 (MH⁺, 75), C₁₂H₁₂ClNO₃: 253.7. Specific optical rotation [α]_D²⁵ +79 (c 0.02, CH₃OH). Anal. Calcd for C₁₂H₁₂ClNO₃: C, 56.81; H, 4.77; Cl, 13.98; N, 5.52; O, 18.92. Found: C, 56.72; H, 4.76; Cl, 13.96; N, 5.50; O, 18.89. Overall yield 14%.

5.2.7. General procedures for coupling of Fmoc-D/L-Glu-(OAll)-OH to Rink amide resin

Example: Synthesis of (R)-15.

0.12 mmol of Rink amide resin (Novabiochem) previously Fmoc-deprotected (double treatment of the resin with piperidine 20% in DMF) were swollen in DCM.

A solution of Fmoc-D-Glu-(OAll)-OH (R)-11 (0.24 g, 0.59 mmol), 2-(1H-benzotriazole-1-yl)-1,1,3,3-tetramethyluronium hexafluorophosphate (HBTU) (0.22 g, 0.59 mmol), *N*-hydroxybenzotriazole (HOBT) (80 mg, 0.59 mmol), and *N*-methylmorpholine (NMM) (130 μ l, 1.18 mmol) in 1 ml dry DMF was introduced into the cartridge. After stirring at room temperature for 2 h, the resin was filtered, rinsed with DMF (3 × 5 ml), DCM (3 × 5 ml) and TBME (3 × 5 ml) and finally dried in vacuo.

A positive Kaiser test²⁷ resulted, indicating no free amine groups on the resin.

5.2.8. General procedures for Fmoc deprotection and reductive amination of polymer bound O-all-glutamate

The same procedure described for NovaSynTGOH bound derivatives (Synthesis of (R)-13) was followed.

5.2.9. General procedures for synthesis of polymer bound pyroglutamate ring

The same procedure described for NovaSynTGOH bound derivatives (synthesis of (R)-14a) was followed.

5.2.10. General procedures for the cleavage of carboxamide derivatives 1''

Example: (R)-1-(4-chlorobenzyl)-5-oxopyrrolidine-2-carboxamide [(R)-1'c].

(R)-17c was subject to cleavage by treatment with TFA/TIS (95:5) (120 μ l, 2 mmol) in order to obtain (R)-1'c carboxamide. After rocking for 1 h at room temperature, the resin was filtered and the filtrate was evaporated to dryness.

The crude compound (R)-1'c did not need further purification as shown by HPLC–MS analysis (97% of pure compound at 220 nm; 88% at 254 nm).

Waxy solid—¹H NMR (300 MHz, DMSO-*d*₆): δ 1.79–1.89 (m, 1H), 2.05–2.37 (m, 3H), 3.73 (d, 1H, *J* = 15.2 Hz), 3.85 (dd, 1H, *J* = 8.8, 3.42 Hz), 4.81 (d, 1H, *J* = 15.2 Hz), 7.16 (br s, 1H), 7.21 (d, 2H, *J* = 8.3 Hz), 7.39 (d, 2H, *J* = 8.3 Hz), 7.55 (br s, 1H). LC–MS (ESI) (H₂O/CH₃CN, 1%TFA) *m/z* (%): 253.2 (MH⁺, 100), C₁₂H₁₃ClN₂O₂: 252.1. Specific optical rotation [α]_D²⁵ –56 (c 0.04, CH₃OH). Anal. Calcd for C₁₂H₁₃ClN₂O₂: C, 57.04; H, 5.19; Cl, 14.03; N, 11.09; O, 12.66. Found: C, 57.14; H, 5.20; Cl, 14.05; N, 11.11; O, 12.69. Overall yield 32%.

5.2.10.1. (R)-1'a: (R)-1-(4-Phenylbenzyl)-5-oxopyrrolidine-2-carboxamide.

Waxy solid—¹H NMR (300 MHz, DMSO-*d*₆): δ 1.81–1.89 (m, 1H), 2.07–2.42 (m, 3H), 3.74 (d, 1H, *J* = 15.3 Hz), 3.91 (dd, 1H, *J* = 9.0, 3.09 Hz), 4.93 (d, 1H, *J* = 15.3 Hz), 7.19 (s, 1H), 7.28 (d, 2H, *J* = 8.2 Hz), 7.36 (t, 1H, *J* = 7.4 Hz), 7.46 (t, 2H, *J* = 7.8 Hz), 7.58 (s, 1H), 7.63 (d, 2H, *J* = 7.8 Hz), 7.65 (d, 2H, *J* = 6.6 Hz). LC–MS (ESI) (H₂O/CH₃CN, 1%TFA) *m/z* (%): 295.2 (MH⁺,

100), C₁₈H₁₈N₂O₂: 294.3. Specific optical rotation $[\alpha]_D^{25}$ –66 (c 0.03, CH₃OH). Anal. Calcd for C₁₈H₁₈N₂O₂: C, 73.45; H, 6.16; N, 9.52; O, 10.87. Found: C, 73.20; H, 6.17; N, 9.54; O, 10.83. Overall yield 34%.

5.2.10.2. (S)-1^a: (S)-1-(4-Phenylbenzyl)-5-oxopyrrolidine-2-carboxamide. Waxy solid—¹H NMR (300 MHz, DMSO-*d*₆): δ 1.80–1.89 (m, 1H), 2.06–2.41 (m, 3H), 3.73 (d, 1H, *J* = 15.3 Hz), 3.91 (dd, 1H, *J* = 9.0, 3.91 Hz), 4.91 (d, 1H, *J* = 15.3 Hz), 7.19 (s, 1H), 7.27 (d, 2H, *J* = 7.8 Hz), 7.35 (t, 1H, *J* = 7.4 Hz), 7.46 (t, 2H, *J* = 7.4 Hz), 7.60 (s, 1H), 7.63 (t, 4H, *J* = 6.6 Hz). LC–MS (ESI) (H₂O/CH₃CN, 1%TFA) *m/z* (%): 295.2 (MH⁺, 100), C₁₈H₁₈N₂O₂: 294.3. Specific optical rotation $[\alpha]_D^{25}$ +69 (c 0.04, CH₃OH). Anal. Calcd for C₁₈H₁₈N₂O₂: C, 73.45; H, 6.16; N, 9.52; O, 10.87. Found: C, 73.30; H, 6.17; N, 9.53; O, 10.85. Overall yield 37%.

5.2.10.3. (R)-1^b: (R)-1-(2-Chlorobenzyl)-5-oxopyrrolidine-2-carboxamide. Waxy solid—¹H NMR (300 MHz, DMSO-*d*₆): δ 1.82–1.91 (m, 1H), 2.07–2.37 (m, 3H), 3.89–3.95 (m, 2H), 4.84 (d, 1H, *J* = 16.1 Hz), 7.16 (br s, 1H), 7.24 (t, 1H, *J* = 4.4 Hz), 7.33 (t, 2H, *J* = 4.4 Hz), 7.46 (t, 1H, *J* = 4.4 Hz), 7.54 (br s, 1H). LC–MS (ESI) (H₂O/CH₃CN, 1%TFA) *m/z* (%): 253.2 (MH⁺, 100), C₁₂H₁₃ClN₂O₂: 252.1. Specific optical rotation $[\alpha]_D^{25}$ –89 (c 0.03, CH₃OH). Anal. Calcd for C₁₂H₁₃ClN₂O₂: C, 57.04; H, 5.19; Cl, 14.03; N, 11.09; O, 12.66. Found: C, 56.95; H, 5.18; Cl, 13.98; N, 11.06; O, 12.62. Overall yield 33%.

5.2.10.4. (S)-1^b: (S)-1-(2-Chlorobenzyl)-5-oxopyrrolidine-2-carboxamide. Waxy solid—¹H NMR (300 MHz, DMSO-*d*₆): δ 1.82–1.90 (m, 1H), 2.07–2.37 (m, 3H), 3.89–3.92 (m, 1H), 3.93 (d, 1H, *J* = 15.6 Hz), 4.84 (d, 1H, *J* = 15.6 Hz), 7.17 (br s, 1H), 7.24 (t, 1H, *J* = 4.9 Hz), 7.33 (t, 2H, *J* = 4.4 Hz), 7.46 (t, 1H, *J* = 4.9 Hz), 7.54 (br s, 1H). LC–MS (ESI) (H₂O/CH₃CN, 1%TFA) *m/z* (%): 253.1 (MH⁺, 100), C₁₂H₁₃ClN₂O₂: 252.1. Specific optical rotation $[\alpha]_D^{25}$ +91 (c 0.05, CH₃OH). Anal. Calcd for C₁₂H₁₃ClN₂O₂: C, 57.04; H, 5.19; Cl, 14.03; N, 11.09; O, 12.66. Found: C, 57.01; H, 5.18; Cl, 13.99; N, 11.07; O, 12.64. Overall yield 34%.

5.2.10.5. (S)-1^c: (S)-1-(4-Chlorobenzyl)-5-oxopyrrolidine-2-carboxamide. Waxy solid—¹H NMR (300 MHz, DMSO-*d*₆ + D₂O): δ 1.77–1.85 (m, 1H), 2.14–2.41 (m, 3H), 3.74 (d, 1H, *J* = 15.2 Hz), 3.89 (dd, 1H, *J* = 8.8, 3.91 Hz), 4.75 (d, 1H, *J* = 15.2 Hz), 7.17 (d, 2H, *J* = 8.3 Hz), 7.35 (d, 2H, *J* = 8.3 Hz). LC–MS (ESI) (H₂O/CH₃CN, 1%TFA) *m/z* (%): 253.1 (MH⁺, 100), C₁₂H₁₃ClN₂O₂: 252.1. Specific optical rotation $[\alpha]_D^{25}$ +55 (c 0.03, CH₃OH). Anal. Calcd for C₁₂H₁₃ClN₂O₂: C, 57.04; H, 5.19; Cl, 14.03; N, 11.09; O, 12.66. Found: C, 57.10; H, 5.20; Cl, 14.04; N, 11.11; O, 12.67. Overall yield 31%.

5.2.11. General procedures for loading Fmoc-NHOH on chlorotriptylresin

Example: Synthesis of 19.

A solution of Fmoc-NHOH (51 mg, 0.2 mmol) and DIPEA (70 μl, 0.4 mmol) in 2 ml DCM was dropped on chlorotriptyl resin (Nova-biochem) (0.2 mmol) pre-swollen in DCM.²⁸

After shaking for 60 h at room temperature, the resin was filtered and rinsed with DCM (3 × 5 ml) DMF (3 × 5 ml), DCM (3 × 5 ml) and TBME (3 × 5 ml) and finally dried in vacuo.

The efficiency of loading (loading yield: 53%) was determined on 3 mg of resin by Fmoc removal analysis (treatment of the resin with piperidine 20% in DMF) and absorbance measurement at 301 nm (UV–vis Spectrophotometer Shimadzu).

5.2.12. General procedures for coupling of proline/thioproline/hydroxyproline rings to -NHOH functionalized resin

Example: Synthesis of 23.

A solution of Fmoc-L-proline (0.34 g, 1 mmol), HATU (0.38 g, 1 mmol), and DIPEA (348 μl, 2 mmol) in 2 ml of dry DMF/DCM (1:1) was added dropwise on the functionalized resin **19** (0.2 mmol) after Fmoc deprotection via classical procedure (20% Piperidine in DMF for 20 min (×2)). The cartridge was shaken for 12 h at room temperature.

After filtration the resin was rinsed with DMF (3 × 5 ml), DCM (3 × 5 ml) and TBME (3 × 5 ml) and finally dried in vacuo.

The efficiency of loading (loading yield: 53%) was determined on 3 mg of resin by Fmoc removal analysis (treatment of the resin with piperidine 20% in DMF) and absorbance measurement at 301 nm (UV–vis Spectrophotometer Shimadzu).

5.2.13. General procedures for Fmoc deprotection and reductive amination on polymer bound proline/thioproline/hydroxyproline rings

The same procedure described for the synthesis of (R)-**13** was followed.

5.2.14. General procedures for cleavage of hydroxamates derivatives 2a, 3a, 4a

Example: Synthesis 2a.

After swelling functionalized resin **26**, the crude product **2a** (0.1 mmol) was cleaved by treatment with 2 ml of AcOH/TFE/DCM (1:1:8) for 1 h at room temperature. The resin was filtered and the filtrate was evaporated under N₂.

The crude product **2a** was further purified by semi-preparative RP-HPLC (C18, Nucleosil 300 mm × 25 mm, 3 ml/min, detection at 230 nm, eluent A: Water/TFA: 99.92:0.08, eluent B: acetonitrile/TFA: 99.92:0.08; gradient B from 20% to 80% in 14 min, from 80% to 98% in 3 min).

¹H NMR (300 MHz, DMSO-*d*₆): waxy solid—¹H NMR (300 MHz, DMSO-*d*₆): δ 1.77–1.94 (m, 2H), 2.00–2.13 (m, 1H), 3.14–3.35 (m, 1H), 3.93–4.04 (m, 1H), 4.10–4.20 (m, 1H), 4.25–4.45 (m, 3H), 7.38–7.77 (m, 9H), 9.31 (br s, 1H), 11.12 (br s, 1H). LC–MS (ESI) (H₂O/CH₃CN, 1%TFA) *m/z* (%): 297.3 (MH⁺, 100), C₁₈H₂₀N₂O₂: 296.1. Specific optical rotation $[\alpha]_D^{25}$ –17 (c 0.02, CH₃OH). Anal. Calcd for C₁₈H₂₀N₂O₂: C, 72.95; H, 6.80; N, 9.45; O, 10.80. Found: C, 73.98; H, 6.79; N, 9.46; O, 10.77. Overall yield 22%.

5.2.14.1. Compound 3a. Waxy solid—¹H NMR (300 MHz, DMSO-*d*₆): δ 3.10 (s, 3H), 3.89–3.91 (m, 1H), 3.95–4.00 (m, 1H), 4.06–4.09 (m, 1H), 4.23–4.28 (m, 1H), 4.44–4.47 (m, 1H), 7.37–7.70 (m, 9H), 9.88–9.99 (m, 1H), 11.26 (br s, 1H). LC–MS (ESI) (H₂O/CH₃CN, 1%TFA) *m/z* (%): 315.2 (MH⁺, 100), C₁₇H₁₈N₂O₂S: 314.1.

Specific optical rotation $[\alpha]_D^{25}$ –8 (c 0.06, CH₃OH). Anal. Calcd for C₁₇H₁₈N₂O₂S: C, 64.94; H, 5.77; N, 8.91; O, 10.18; S, 10.20. Found: C, 64.71; H, 5.76; N, 8.93; O, 10.22; S, 10.25. Overall yield 20%.

5.2.14.2. 4a: (2S,4R)-N,4-Dihydroxy-1-benzyl(4'-phenyl)-pyrrolidine-2-carboxamide.

Waxy solid—¹H NMR (300 MHz, DMSO-*d*₆): δ 1.99–2.10 (m, 1H), 2.15–2.27 (m, 1H), 3.03–3.17 (m, 1H), 3.55–3.70 (m, 2H), 4.10–4.20 (m, 1H), 4.33–4.49 (m, 3H), 7.38–7.76 (m, 9H), 9.29 (br s, 1H), 11.06 (br s, 1H). LC–MS (ESI) (H₂O/CH₃CN, 1%TFA) *m/z* (%): 313.2 (MH⁺, 100), C₁₈H₂₀N₂O₃: 312.5.

Specific optical rotation $[\alpha]_D^{25}$ –2 (c 0.1, CH₃OH). Anal. Calcd for C₁₈H₂₀N₂O₃: C, 69.21; H, 6.45; N, 8.97; O, 15.37. Found: C, 69.10; H, 6.43; N, 8.79; O, 15.40. Overall yield 27%.

5.2.15. General procedures for coupling of Fmoc-D-Cys-(trt)-OH to NovaSynTGOH resin

A solution of Fmoc-D-Cys-(trt)-OH (1.02 g, 1.7 mmol), HATU (0.65 g, 1.7 mmol), and DIEA (600 μl, 3.4 mmol) in 3 ml of dry DMF was dropped on the resin NovaSynTGOH (1.12 g, 0.34 mmol).

DMAP (8.5 mg, 0.2 mmol) in 0.5 ml of dry DMF was added, and the cartridge was shaken at room temperature for 6 h.

After filtration of the solution the resin was rinsed with DMF (3 × 5 ml), DCM (3 × 5 ml) and TBME (3 × 5 ml) and finally dried in vacuo.

The efficiency of loading (loading yield: 80%) was determined on 8.3 mg of resin by Fmoc removal analysis (treatment of the resin with piperidine 20% in DMF) and absorbance measurement at 301 nm (UV–vis Spectrophotometer Shimadzu).

5.2.16. General procedures for Fmoc deprotection and reductive amination

The same procedure described for the synthesis of (R)-13 was followed.

5.2.17. General procedures for trityl deprotection and cyclization

Trityl deprotection of 31 (0.04 mmol pre-swollen in DCM) was performed with TFA/triisopropyl silane (TIS)/DCM 10:5:85 (4 × 30 min). Then the resin was filtered, rinsed with DCM and a solution of 10% Et₃N in DMF was added.

After filtering and washing (DMF, DCM), a solution of CDI (60 mg, 0.37 mmol) dissolved in 1 ml dry DCM was introduced into the cartridge; the cyclization proceeded for 6 h at room temperature. Functionalized resin 32 was then rinsed with DCM (×3), DMF (×3), DCM (×3), and TBME (×3).

5.2.18. General procedures for the cleavage of hydroxamate derivatives 5a

The same procedure described for (R)-1a was followed.

Compound 5a: Amorphous solid—¹H NMR (300 MHz, DMSO-*d*₆): δ 3.19–3.24 (m, 1H), 3.60 (dd, 1H, *J* = 8.6, 10.9 Hz), 3.83 (d, 1H, *J* = 15.1 Hz), 4.09–4.19 (m, 1H), 4.89 (d, 1H, *J* = 15.7 Hz), 7.28–7.41 (m, 3H), 7.42–7.51 (m, 2H), 7.66 (d, 4H *J* = 8.1 Hz), 9.21 (s, 1H), 10.89 (s, 1H). LC–MS (ESI) (H₂O/CH₃CN, 1%TFA) *m/z* (%): 329.2 (MH⁺, 10), C₁₇H₁₈N₂O₆S₂: 328.4. Specific optical rotation [α]_D²⁵ –37 (c 0.03, CH₃OH). Anal. Calcd for C₁₇H₁₆N₂O₃S: C, 62.18; H, 4.91; N, 8.53; O, 14.62; S, 9.76. Found: C, 62.16; H, 4.87; N, 8.58; O, 14.64; S, 9.78. Overall yield 35%.

5.2.19. General procedure for synthesis of Fmoc-D-Glu(OAll)-NH₂ and loading on chlorotriptyl resin

A solution of Fmoc-D-Glu-(OAll) chloride (obtained by the reaction between Fmoc-D-Glu-(OAll)-OH (0.32 g, 0.77 mmol) and SOCl₂ (1.5 ml, 21 mmol) in dioxane for 2.5 h at 50 °C) in 1 ml of dioxane was added to a freshly prepared solution of hydroxylamine, obtained by reaction between hydroxylamine hydrochloride (0.27 g, 3.85 mmol) and DIEA (690 μl, 3.85 mmol) in dioxane/water. After being stirred at room temperature overnight, the mixture was evaporated under reduced pressure and DCM and HCl 0.1 M solution were added. The organic layer was separated, and the aqueous one was extracted with DCM (2 × 5 mL). The combined organic solutions were dried (MgSO₄), and evaporated to dryness.

A solution of the pure compound 33 (95.7% 220 nm, 91.2% 254 nm) (0.15 mg, 0.35 mmol) and DIEA (165 μl, 0.92 mmol) in 3 ml DMF/DCM (1:10) was added dropwise on chlorotriptyl resin (Novabiochem) (160 mg, 0.23 mmol) pre-swollen in DCM. After shaking for 60 h at room temperature, the resin was filtered and rinsed first with DCM/MeOH/DIEA (17:2:1) (3 × 5 min) and later with DCM (3 × 5 ml), DMF (3 × 5 ml), DCM (3 × 5 ml) and TBME (3 × 5 ml) and finally dried in vacuo. The efficiency of loading (loading yield: 60%) was determined on 2.8 mg of resin by Fmoc removal analysis (treatment of the resin with piperidine 20% in DMF) and absorbance measurement at 301 nm (UV–vis Spectrophotometer Shimadzu).

5.2.20. General procedures for Fmoc deprotection and N-sulphonylation

After Fmoc deprotection of (R)-34 with 20% piperidine in DMF for 20 min (×2), the resin (70 mg, 0.07 mmol) was washed (2 × DMF, 2 × DCM), and DIEA (0.41 mmol, 73 μl) and a solution of bisphenylsulfonfyl chloride (0.27 mmol, 68 mg) in 1.5 ml of dry DCM (11 mg, 0.09 mmol) were added dropwise. After shaking overnight at room temperature, the resin was filtered and rinsed with DCM (×3), DMF (×3), DCM (×3) and TBME (×3).

5.2.21. General procedures for allyl deprotection and cyclization

The same procedure described for (R)-14 was followed.

5.2.22. General procedures for cleavage of hydroxamates 6a

The crude product 6a was cleaved by treatment of 36a with 2.5 ml of TFA (5%) in DCM for 2 h at room temperature. The resin was then filtered and filtrate was evaporated under N₂.

6a was further purified by semi-preparative RP-HPLC (C18, Nucleosil 300 mm × 25 mm, 3 ml/min, detection at 230 nm, eluent A: Water/TFA: 99.92:0.08, eluent B: acetonitrile/TFA: 99.92:0.08; gradient B from 20% to 80% in 14 min, from 80% to 98% in 3 min).

Amorphous solid—¹H NMR (300 MHz, DMSO-*d*₆): δ 1.84–1.97 (m, 1H), 2.23–2.49 (m, 3H), 4.67 (d, 1H, *J* = 8.1 Hz), 7.42–7.59 (m, 3H), 7.7 (d, 2H, *J* = 7.6 Hz), 7.91 (d, 2H *J* = 8.7 Hz), 8.04 (d, 2H *J* = 8.7 Hz), 9.18 (s, 1H), 11 (s, 1H). LC–MS (ESI) (H₂O/CH₃CN, 1%TFA) *m/z* (%): 361.2 (MH⁺, 75), C₁₇H₁₆N₂O₅S: 360.4. Specific optical rotation [α]_D²⁵ +11 (c 0.02, CH₃OH). Anal. Calcd for C₁₇H₁₆N₂O₅S: C, 56.66; H, 4.47; N, 7.77; O, 22.20; S, 8.90. Found: C, 56.55; H, 4.49; N, 7.80; O, 22.22; S, 8.92. Overall yield 12%.

5.2.23. General procedure for synthesis of series 7, 8, 9, 10

The synthesis of 7, 8 series was realized according to a common parallel strategy except for the coupling to NovaSynTGOH resin: N-Fmoc proline and N-Fmoc thioproline were loaded respectively via HATU and via fluoride. The subsequent synthetic steps were performed with the same experimental procedures.

5.2.24. General procedures for coupling of N-Fmoc proline to NovaSynTGOH

Example: Synthesis of 37.

A solution of Fmoc-L-proline (0.34 g, 1 mmol), HATU (0.38 g, 1 mmol), and DIPEA (348 μl, 2 mmol) in 2 ml of dry DMF/DCM (1:1) was dropped on the resin NovaSynTGOH (0.2 mmol).

The cartridge was rocked 12 h at room temperature.

After filtration the resin was rinsed with DMF (3 × 5 ml), DCM (3 × 5 ml) and TBME (3 × 5 ml) and finally dried in vacuo.

The efficiency of loading (loading yield: 80%) was determined on 8.3 mg of resin by Fmoc removal analysis (treatment of the resin with piperidine 20% in DMF) and absorbance measurement at 301 nm (UV–vis Spectrophotometer Shimadzu).

5.2.25. General procedures for coupling of N-Fmoc thiazolidine to NovaSynTGOH

Example: Synthesis of 38.

A solution of N-Fmoc thiazolidine (0.34 g, 1 mmol), HATU (0.38 g, 1 mmol), and DIPEA (348 μl, 2 mmol) in 2 ml of dry DMF/DCM (1:1) was added dropwise on was added to NovaSynTGOH (0.2 mmol) after Fmoc deprotection via classical procedure (20% Piperidine in DMF for 20 min (×2)). The cartridge was shaken for 12 h at room temperature.

After filtration the resin was rinsed with DMF (3 × 5 ml), DCM (3 × 5 ml) and TBME (3 × 5 ml) and finally dried in vacuo.

The efficiency of loading (loading yield: 53%) was determined on 3 mg of resin by Fmoc removal analysis (treatment of the resin with piperidine 20% in DMF) and absorbance measurement at 301 nm (UV–vis Spectrophotometer Shimadzu).

5.2.26. General procedures for *N*-sulphonylation of polymer bound proline/thioproline

Example: Synthesis of **40a**.

After Fmoc deprotection with 20% piperidine in DMF for 20 min ($\times 2$), **39** (0.03 mmol) was washed ($2 \times$ DMF, $2 \times$ DCM) and pre-swollen in 2 ml of THF in presence of DMAP (3.4 mg, 0.03 mmol). A solution of bisphenylsulphonylchloride (0.14 mmol) in 1 ml of dry DCM was added and the cartridge was rocked for 12 h at room temperature.

Then the resin was filtered and washed with MeOH ($\times 2$), DMF ($\times 2$), DCM ($\times 2$) and TBME ($\times 2$).

5.2.27. General procedures for cleavage of hydroxamate derivatives **7**, **8**

Example: Synthesis of **8a**.

Functionalized resin derivative **40a** (0.03 mmol) was swollen in THF (1.8 ml) and cleaved by solid support by treatment with 50% NH_2OH in H_2O (300 μl , 5.6 mmol). After rocking for 5 h at room temperature, the resin was filtered and the filtrate was evaporated to dryness.

The crude product **8a** was further purified by semi-preparative RP-HPLC (C18, Nucleosil 300 mm \times 25 mm, 3 ml/min, detection at 230 nm, eluent A: Water/TFA: 99.92:0.08, eluent B: acetonitrile/TFA: 99.92:0.08; gradient B from 20% to 80% in 14 min, from 80% to 98% in 3 min).

5.2.27.1. Compound 8a. Amorphous solid— ^1H NMR (300 MHz, $\text{DMSO}-d_6$): δ 2.83–2.93 (m, 1H), 2.97–3.04 (m, 1H), 4.46 (d, 1H, $J = 10.8$ Hz), 4.52 (dd, 1H, $J = 5.9, 7.57$ Hz), 4.85 (d, 1H, $J = 10.8$ Hz), 7.44–7.57 (m, 3H), 7.79 (d, 2H, $J = 7.6$ Hz), 7.91–8.03 (m, 4H), 9.05 (s, 1H), 10.87 (s, 1H). LC–MS (ESI) ($\text{H}_2\text{O}/\text{CH}_3\text{CN}$, 1%TFA) m/z (%): 365.2 (MH^+ , 100), $\text{C}_{16}\text{H}_{16}\text{N}_2\text{O}_4\text{S}_2$: 364.4. Specific optical rotation $[\alpha]_{\text{D}}^{25} -125$ (c 0.03, CH_3OH). Anal. Calcd for $\text{C}_{16}\text{H}_{16}\text{N}_2\text{O}_5\text{S}$: C, 50.51; H, 4.24; N, 7.36; O, 21.03; S, 16.86. Found: C, 50.60; H, 4.25; N, 7.41; O, 21.06; S, 16.90. Overall yield 34%.

5.2.27.2. Compound 7a. Amorphous solid— ^1H NMR (300 MHz, $\text{DMSO}-d_6$): δ 1.45–1.58 (m, 1H), 1.67–1.93 (m, 3H), 3.14–3.26 (m, 1H), 3.38–3.49 (m, 1H), 3.98 (dd, 1H, $J = 4.4, 8.12$ Hz), 7.44–7.57 (m, 3H), 7.77 (d, 2H, $J = 7.6$ Hz), 7.93 (s, 4H), 8.95 (s, 1H), 10.70 (s, 1H). LC–MS (ESI) ($\text{H}_2\text{O}/\text{CH}_3\text{CN}$, 1%TFA) m/z (%): 347.2 (MH^+ , 45), $\text{C}_{17}\text{H}_{18}\text{N}_2\text{O}_4\text{S}$: 346.4. Specific optical rotation $[\alpha]_{\text{D}}^{25} -110$ (c 0.04, CH_3OH). Anal. Calcd for: $\text{C}_{17}\text{H}_{18}\text{N}_2\text{O}_4\text{S}$: C, 58.94; H, 5.24; N, 8.09; O, 18.48; S, 9.26. Found: C, 58.88; H, 5.21; N, 8.12; O, 18.50; S, 9.21. Overall yield 38%.

5.2.27.3. Compound 8h. Amorphous solid— ^1H NMR (300 MHz, $\text{DMSO}-d_6$): δ 2.75–2.83 (m, 1H), 2.98 (dd, 1H, $J = 5.4, 11.36$ Hz), 4.47 (d, 1H, $J = 10.8$), 4.57 (dd, 1H, $J = 5.4, 7.03$ Hz), 4.9 (d, 3H), 7.67–7.79 (m, 2H), 7.90–7.96 (m, 1H), 8.05–8.23 (m, 3H), 8.60 (s, 1H), 8.71 (s, 1H), 9.11 (s, 1H). LC–MS (ESI) ($\text{H}_2\text{O}/\text{CH}_3\text{CN}$, 1%TFA) m/z (%): 339.2 (MH^+ , 100), $\text{C}_{14}\text{H}_{14}\text{N}_2\text{O}_4\text{S}_2$: 338.4. Specific optical rotation $[\alpha]_{\text{D}}^{25} -80$ (c 0.06, CH_3OH). Anal. Calcd for $\text{C}_{14}\text{H}_{14}\text{N}_2\text{O}_5\text{S}_2$: C, 47.45; H, 3.98; N, 7.90; O, 22.57; S, 18.10. Found: C, 47.42; H, 4.00; N, 7.99; O, 22.49; S, 18.12. Overall yield 35%.

5.2.27.4. 8i-TFA salt. Amorphous solid— ^1H NMR (300 MHz, $\text{DMSO}-d_6$): δ 2.80–2.89 (m, 1H), 2.99 (dd, 1H, $J = 3.8, 11.36$ Hz), 4.44 (d, 1H, $J = 9.7$), 4.95 (d, 1H, $J = 9.7$ Hz), 5.27 (dd, 1H, $J = 4.3, 7.6$ Hz), 7.72–7.84 (m, 2H), 8.37 (d, 1H, $J = 8.1$ Hz), 8.46 (d, 1H, $J = 7.0$ Hz), 8.58 (d, 1H, $J = 8.1$ Hz), 9.09 (d, 1H, $J = 4.3$ Hz), 10.75 (s, 1H), 11.05 (s, 1H), 12.19 (s, 1H). LC–MS (ESI) ($\text{H}_2\text{O}/\text{CH}_3\text{CN}$, 1%TFA) m/z (%): 340.2 ($\text{MH}^+ - \text{CF}_3\text{CO}_2^-$, 100), $\text{C}_{15}\text{H}_{14}\text{F}_3\text{N}_3\text{O}_6\text{S}_2$: 453.4. Specific optical rotation $[\alpha]_{\text{D}}^{25} -66$ (c 0.05, CH_3OH). Anal. Calcd for $\text{C}_{15}\text{H}_{14}\text{F}_3\text{N}_3\text{O}_7\text{S}_2$: C, 38.38; H, 3.01; F, 12.14; N, 8.95; O,

23.86; S, 13.66. Found: C, 38.41; H, 3.01; F, 12.16; N, 8.98; O, 23.90; S, 13.63. Overall yield 25%.

5.2.27.5. Compound 8j. Amorphous solid— ^1H NMR (300 MHz, $\text{DMSO}-d_6$): δ 2.81–2.88 (m, 1H), 3.0 (dd, 1H, $J = 5.4, 11.90$ Hz), 4.39–4.49 (m, 2H), 4.75 (d, 1H, $J = 10.8$ Hz), 7–7.08 (m, 4H), 7.13 (d, 2H, $J = 9.2$ Hz), 7.87 (d, 2H, $J = 8.7$ Hz), 9.07 (br s, 2H). LC–MS (ESI) ($\text{H}_2\text{O}/\text{CH}_3\text{CN}$, 1%TFA) m/z (%): 411.1 (MH^+ , 45), $\text{C}_{17}\text{H}_{18}\text{N}_2\text{O}_6\text{S}_2$: 410.5. Specific optical rotation $[\alpha]_{\text{D}}^{25} -22$ (c 0.1, CH_3OH). Anal. Calcd for $\text{C}_{17}\text{H}_{18}\text{N}_2\text{O}_7\text{S}_2$: C, 47.88; H, 4.25; N, 6.57; O, 26.26; S, 15.04. Found: C, 47.81; H, 4.26; N, 6.51; O, 26.23; S, 15.05. Overall yield 29%.

5.2.27.6. Compound 8k. Amorphous solid— ^1H NMR (300 MHz, $\text{DMSO}-d_6$): δ 2.70–2.80 (m, 1H), 2.98–3.05 (m, 1H), 4.40–4.52 (m, 2H), 4.72 (d, 1H, $J = 10.3$ Hz), 7.09–7.24 (m, 4H), 7.53 (d, 2H, $J = 8.7$ Hz), 7.91 (d, 2H, $J = 8.7$ Hz), 8.61–8.93 (br s, 2H). LC–MS (ESI) ($\text{H}_2\text{O}/\text{CH}_3\text{CN}$, 1%TFA) m/z (%): 415.1 (MH^+ , 90), $\text{C}_{16}\text{H}_{15}\text{ClN}_2\text{O}_5\text{S}_2$: 414.9. Specific optical rotation $[\alpha]_{\text{D}}^{25} -21$ (c 0.1, CH_3OH). Anal. Calcd for $\text{C}_{16}\text{H}_{15}\text{ClN}_2\text{O}_6\text{S}_2$: C, 44.60; H, 3.51; Cl, 8.23; N, 6.50; O, 22.28; S, 14.88. Found: C, 45.58; H, 3.52; Cl, 8.21; N, 6.51; O, 22.26; S, 14.86. Overall yield 35%.

5.2.27.7. Compound 8l. Amorphous solid— ^1H NMR (300 MHz, $\text{DMSO}-d_6$): δ 2.70 (dd, 1H, $J = 7.6, 10.8$ Hz), 3.10 (dd, 1H, $J = 3.2, 10.8$ Hz), 4.36 (d, 1H, $J = 10.3$ Hz), 4.66–4.75 (m, 2H), 7.05–7.14 (m, 2H), 7.18–7.36 (m, 4H), 7.86–7.93 (m, 2H), 8.75 (s, 1H), 8.87 (s, 1H). LC–MS (ESI) ($\text{H}_2\text{O}/\text{CH}_3\text{CN}$, 1%TFA) m/z (%): 399.1 (MH^+ , 100), $\text{C}_{16}\text{H}_{15}\text{FN}_2\text{O}_5\text{S}_2$: 398.4. Specific optical rotation $[\alpha]_{\text{D}}^{25} -18$ (c 0.07, CH_3OH). Anal. Calcd for $\text{C}_{16}\text{H}_{15}\text{FN}_2\text{O}_6\text{S}_2$: C, 46.37; H, 3.65; F, 4.58; N, 6.76; O, 23.16; S, 15.47. Found: $\text{C}_{16}\text{H}_{15}\text{FN}_2\text{O}_6\text{S}_2$: C, 46.42; H, 3.65; F, 4.57; N, 6.78; O, 23.20; S, 15.45. Overall yield 30%.

5.2.28. General procedures for synthesis of oxidized derivatives **41**

Example: Synthesis of **41a**.

MCPBA (31 mg, 0.17 mmol) in 4 ml of dry DCM was added to a DCM pre-swollen **40a** (0.13 mmol) at 0 °C. After rocking for 27 h at room temperature, the resin was filtered and washed with DCM ($\times 2$), DMF ($\times 2$), DCM ($\times 2$) and TBME ($\times 2$) and finally dried in vacuo.

5.2.29. General procedures for synthesis of oxidized derivatives **42**

Example: Synthesis of **42a**.

MCPBA (37 mg, 0.213 mmol) in 4 ml of dry DCM was added to a DCM pre-swollen **41a** (0.04 mmol) at 0 °C. After rocking for 27 h at room temperature, the resin was filtered and washed with DCM ($\times 2$), DMF ($\times 2$), DCM ($\times 2$) and TBME ($\times 2$) and finally dried in vacuo.

5.2.30. General procedures for cleavage of hydroxamate derivatives **9** and **10**

We follow the same procedure described for **8a**.

5.2.30.1. Compound 9a. Amorphous solid— ^1H NMR (300 MHz, $\text{DMSO}-d_6$): δ 2.96 (dd, 1H, $J = 3.8, 13.5$ Hz), 3.17 (dd, 1H, $J = 8.7, 13.5$ Hz), 4.17 (d, 1H, $J = 11.9$ Hz), 4.72 (dd, 1H, $J = 3.8, 8.7$ Hz), 5.30 (d, 1H, $J = 11.9$ Hz), 7.42–7.58 (m, 3H), 7.79 (d, 2H, $J = 7.0$ Hz), 7.97 (m, 4H), 9.12 (s, 1H), 10.89 (s, 1H). LC–MS (ESI) ($\text{H}_2\text{O}/\text{CH}_3\text{CN}$, 1%TFA) m/z (%): 381.1 (MH^+ , 100), $\text{C}_{16}\text{H}_{16}\text{N}_2\text{O}_5\text{S}_2$: 380.4. Specific optical rotation $[\alpha]_{\text{D}}^{25} -159$ (c 0.07, CH_3OH). Anal. Calcd for $\text{C}_{16}\text{H}_{16}\text{N}_2\text{O}_6\text{S}_2$: C, 48.47; H, 4.07; N, 7.07; O, 24.21; S, 16.18. Found: C, 48.35; H, 4.06; N, 7.05; O, 24.16; S, 16.14. Overall yield 17%.

5.2.30.2. Compound 10a. Amorphous solid— ^1H NMR (300 MHz, DMSO- d_6): δ 3.51–3.64 (m, 2H), 4.30 (d, 1H, J = 12.4 Hz), 4.91 (d, 1H, J = 12.4 Hz), 5.10 (dd, 1H, J = 4.9, 8.7 Hz), 7.42–7.58 (m, 3H), 7.78 (d, 2H, J = 7.0 Hz), 7.96 (m, 4H), 9.12 (s, 1H), 10.89 (s, 1H). LC–MS (ESI) ($\text{H}_2\text{O}/\text{CH}_3\text{CN}$, 1%TFA) m/z (%): 397.2 (MH^+ , 100), $\text{C}_{16}\text{H}_{16}\text{N}_2\text{O}_6\text{S}_2$: 396.4 Specific optical rotation $[\alpha]_{\text{D}}^{25}$ –46 (c 0.05, CH_3OH). Anal. Calcd for $\text{C}_{16}\text{H}_{16}\text{N}_2\text{O}_7\text{S}_2$: C, 46.59; H, 3.91; N, 6.79; O, 27.15; S, 15.55. Found: C, 46.65; H, 3.90; N, 6.80; O, 27.21; S, 15.59. Overall yield 12%.

5.2.30.3. Compound 10k. Amorphous solid— ^1H NMR (300 MHz, DMSO- d_6): δ 3.24–3.33 (m, 1H), 3.51–6.66 (m, 1H), 4.41 (d, 1H, J = 12.5 Hz), 4.64 (dd, 1H, J = 6.5, 8.12 Hz), 4.95 (d, 1H, J = 13.0 Hz), 7.13–7.24 (m, 4H), 7.52 (d, 2H, J = 9.2 Hz), 7.94 (d, 4H, J = 9.2 Hz), 9.27 (s, 1H), 11.03 (s, 1H). LC–MS (ESI) ($\text{H}_2\text{O}/\text{CH}_3\text{CN}$, 1%TFA) m/z (%): 447.1 (MH^+ , 60), $\text{C}_{16}\text{H}_{15}\text{ClN}_2\text{O}_7\text{S}_2$: 446.8. Specific optical rotation $[\alpha]_{\text{D}}^{25}$ –60 (c 0.05, CH_3OH). Anal. Calcd for $\text{C}_{16}\text{H}_{15}\text{ClN}_2\text{O}_8\text{S}_2$: C, 41.52; H, 3.27; Cl, 7.66; N, 6.05; O, 27.65; S, 13.85. Found: C, 41.48; H, 3.26; Cl, 7.63; N, 6.03; O, 27.59; S, 13.81. Overall yield 9%.

5.3. Enzymatic assay

The enzymatic assays for MMP1, 2, 3, 8, 9, 12, and 14 were based upon the protocol described by Knight et al.²⁹ Active catalytic domains of MMP1, 3, 8, 9, 12, and 14 were purchased from Biomol (Biomol International, Plymouth Meeting) while proMMP2 (from R&D Systems, Inc.) was activated by incubation for 1 h at 37 °C with aminophenylmercuric acetate (APMA) 1 mM final concentration solution.

All enzymatic solutions were then diluted in Tris–HCl assay buffer (Tris/HCl 50 mM, NaCl 0.1 M, CaCl_2 10 mM, 0.05% Brij 35, pH 7.5) in order to obtain final concentrations of the enzymes used in the assay included between 0.5 and 3 nM.

The fluorogenic substrate was Mca-Pro-Leu-Gly-Leu-Dpa-Ala-Arg-NH $_2$ ³⁰ (Biomol Research Laboratories, Inc.) for all tested MMP. The final substrate concentrations performed in assays conditions were in the range of 2–7 μM .

Test compounds were dissolved in dimethyl sulfoxide (DMSO) and diluted with test buffer solution so that no more than 1% DMSO was present. Test compound and enzymes were added to each well of a 96-well plate and allowed to equilibrate for 1 h at 37 °C prior to the addition of substrate. Determinations of fluorescence was performed using a Varian Cary Eclipse spectrofluorimeter (λ_{ex} 328 nm, λ_{em} 393 nm), respectively after addition of fluorogenic substrate (T0) and after 3 h incubation at 37 °C (T3h).

Inhibitors potency was evaluated from the amount of substrate cleavage calculated from fluorescence delta between the two

measurements T0 and T3h, using a range of test compound concentrations (at least six concentrations, each one in duplicate).

From the resulting dose–response curve IC $_{50}$ values (the concentration of inhibitor required to inhibit 50% of the enzyme activity) were calculated from a three-parameter logistic fit of the data (GraphPad Prism version 4.00 for Windows, GraphPad Software, San Diego California USA).

Acknowledgments

The authors thank Drs. Tatiana Guzzo and Teresa Fabiola Miscioscia for their essential support. This work was financed by MIUR (Ministero dell'Istruzione, dell'Università e della Ricerca).

References and notes

- Coussens, L. M.; Werb, Z. *Chem. Biol.* **1996**, *3*, 895.
- Whittaker, M.; Floyd, C. D.; Brown, P.; Gearing, A. J. H. *Chem. Rev.* **1999**, *99*, 2735.
- Baker, A. H.; Edwards, D. R.; Murphy, G. J. *Cell. Sci.* **2002**, *115*, 3719.
- Li, N. G.; Shi, Z. H.; Tang, Y. P.; Duan, J. A. *Curr. Med. Chem.* **2009**, *16*, 3805.
- Aureli, L.; Gioia, M.; Cerbara, I.; Monaco, F.; Fasciglione, G. F.; Marini, S.; Ascenzi, P.; Topai, A.; Coletta, M. *Curr. Med. Chem.* **2008**, *15*, 2192.
- Oshitari, T.; Okuyama, Y.; Miyata, Y.; Kosano, H.; Takahashi, H.; Natsugari, H. *Bioorg. Med. Chem.* **2011**, *19*, 7085.
- Wang, J.; Medina, C.; Radomski, M. W.; Gilmer, J. F. *Bioorg. Med. Chem.* **2011**, *19*, 4985.
- Dorman, G.; Kocsis-Szommer, K.; Spadoni, C.; Ferdinandy, P. *Recent Pat. Cardiovasc. Drug Discov.* **2007**, *2*, 186.
- Renkiewicz, R.; Qiu, L.; Lesch, C.; Sun, X.; Devalaraja, R.; Cody, T.; Kaldjian, E.; Welgus, H.; Bagagi, V. *Arthritis Rheum.* **2003**, *48*, 1742.
- Pavlaki, M.; Zucker, S. *Cancer Met. Rev.* **2003**, *22*, 177.
- Coussens, L. M.; Fingleton, B.; Matrisian, L. M. *Science* **2002**, *295*, 2387.
- Overall, C. M.; Kleinfeld, O. *Nat. Rev. Cancer* **2006**, *6*, 227.
- Nuti, E.; Tuccinardi, T.; Rossello, A. *Curr. Pharm. Des.* **2007**, *13*, 2087.
- Haas, T. L. *Can. J. Physiol. Pharmacol.* **2005**, *83*, 1.
- Sluiter, J. P.; de Kleijn, D. P.; Pasterkamp, G. *Cardiovasc. Res.* **2006**, *69*, 595.
- Deryugina, E. I.; Quigley, J. P. *Cancer Metastasis Rev.* **2006**, *25*, 9.
- Overall, C. M.; Kleinfeld, O. *Br. J. Cancer* **2006**, *94*, 941.
- Higashi, S.; Miyazaki, K. *Biol. Chem.* **2008**, *283*, 10068.
- Berman, H. M.; Westbrook, J.; Feng, Z.; Gilliland, G.; Bhat, T. N.; Weissig, H.; Shindyalov, I. N.; Bourne, P. E. *Nucleic Acids Res.* **2000**, *28*, 235.
- Shindyalov, I. N.; Bourne, P. E. *Protein Eng.* **1998**, *11*, 739.
- MOE: Chemical Computing Group Inc. (2003): 1010 Sherbrooke Street West, Suite 910, Montreal, H3A 2R7, Canada.
- Lipinski, C. A.; Lombardo, F.; Dominy, B. W.; Feeney, P. J. *Adv. Drug Deliv. Rev.* **2001**, *46*, 3.
- Xu, J.; Stevenson, J. J. *Chem. Inf. Comput. Sci.* **2000**, *40*, 1177.
- Oprea, T. I. *J. Comput. Aided Mol. Des.* **2000**, *14*, 251.
- Kiyama, R.; Tamura, Y.; Watanabe, F.; Tsuzuki, H.; Ohtani, M.; Yodo, M. *J. Med. Chem.* **1999**, *42*, 1723.
- DeLano, W.L. The PyMOL molecular graphics system. 2002 (<http://www.pymol.org>).
- Kaiser, E.; Colescott, R. L.; Bossinger, C. D.; Cook, P. I. *Anal. Biochem.* **1970**, *34*, 595.
- Mellor, S. L.; McGuire, C.; Chan, W. C. *Tetrahedron Lett.* **1997**, *38*, 3311.
- Knight, C. G.; Willenbrock, F.; Murphy, G. *FEBS Lett.* **1992**, *296*, 263.
- Will, H.; Atkinson, S. J.; Butler, G. S.; Smith, B.; Murphy, G. *J. Biol. Chem.* **1996**, *271*, 17119.